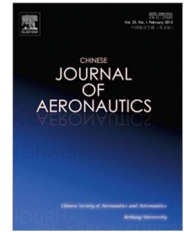




Chinese Society of Aeronautics and Astronautics  
& Beihang University

Chinese Journal of Aeronautics

cja@buaa.edu.cn  
www.sciencedirect.com



## REVIEW

# Ship detection and classification from optical remote sensing images: A survey



Bo LI, Xiaoyang XIE, Xingxing WEI\*, Wenting TANG

*School of Computer Science and Engineering, Beihang University, Beijing 100083, China*

Received 16 June 2020; revised 23 July 2020; accepted 31 August 2020

Available online 14 October 2020

### KEYWORDS

Optical remote sensing;  
Satellite image;  
Sea target detection;  
Ship classification;  
Ship detection

**Abstract** Considering the important applications in the military and the civilian domain, ship detection and classification based on optical remote sensing images raise considerable attention in the sea surface remote sensing filed. This article collects the methods of ship detection and classification for practically testing in optical remote sensing images, and provides their corresponding feature extraction strategies and statistical data. Basic feature extraction strategies and algorithms are analyzed associated with their performance and application in ship detection and classification. Furthermore, publicly available datasets that can be applied as the benchmarks to verify the effectiveness and the objectiveness of ship detection and classification methods are summarized in this paper. Based on the analysis, the remaining problems and future development trends are provided for ship detection and classification methods based on optical remote sensing images.

© 2020 Chinese Society of Aeronautics and Astronautics. Production and hosting by Elsevier Ltd. This is an open access article under the CC BY-NC-ND license (<http://creativecommons.org/licenses/by-nc-nd/4.0/>).

## 1. Introduction

Ship as the key transportation tool on the vast ocean always raises much attention. The application of ship detection and classification provides essential information for strategic decision-making, thus can effectively shorten the decision-making cycle, which is an important basis for real-time battle-field situation awareness in wide range of operational environments.<sup>1–3</sup> With the development of remote sensing imaging technology, the monitoring of the wide-range sea surface has

become possible, which arises extensive research interest in marine target detection and classification technology.<sup>4–6</sup>

Ship detection and classification techniques have great application value in military and civilian domains. In the civil field, it is the basis for implementing the supervision of marine resources, monitoring illegal fishing, and assisting in the maritime rescue, etc.; in the military field, it can be applied to patrols, interests and rights protection in territorial sea region, and monitor important ports, and targets.<sup>4,7</sup> For example, the U.S. Navy undetectably sent the John C. Stennis carrier strike group into the South China Sea and kept radio silence in March 2016 by intentionally close radio communication systems to prevent the detection and identification by the ground electronic radar.<sup>8</sup> If remote sensing monitoring deployed in that circumstance, continue tracking the aircraft carrier battle group is achieved even when the targets are undetectable in other monitoring system.

\* Corresponding author.

E-mail address: [xxwei@buaa.edu.cn](mailto:xxwei@buaa.edu.cn) (X. WEI).

Peer review under responsibility of Editorial Committee of CJA.



Production and hosting by Elsevier

In recent years, with the rapid development of satellite remote sensing imaging technology, ship targets detection and classification from remote sensing images become an important application direction of remote sensing target recognition. Optical remote sensing images are conducive to human visual interpretation, so they are more useful for observing the earth's dynamic surface.<sup>9</sup> Therefore, ship detection and classification based on optical remote sensing images are of main importance in future research and development.

The main contributions of this paper are as follows: (A) a comprehensive review on most popular techniques for both ship detection task and classification task from optical remote sensing images is provided; (B) the publicly available datasets for ship detection and classification on aerial view satellite images are thoroughly collected; (C) experimental results of the state of the art methods for ship detection and classification on publication dataset are compared and discussed; (D) challenges in ship detection and classification from optical remote sensing images and possible futuristic trends are analyzed and discussed.

In this literature, the term 'optical remote sensing images' includes panchromatic remote sensing images (PAN) and multispectral remote sensing images, which mainly contain Blue (B), Green (G), Red (R), Near-Infrared (NIR) bands, additionally, satellite WorldView-2 also contains four new color sensors, Red Edge (RE), Coastal (C), Yellow (Y), and Second Near-Infrared (NIR2) bands. In addition, some multispectral remote sensing images were also included infrared imaging remote sensing images, that are Short-Wavelength Infrared (SWIR), Mid-Wavelength Infrared (MWIR), and Thermal Infrared Sensors (TIRS). As for the notions, 'ship' refers to the man-made objects that sail on the sea surface. As for the term 'object detection' in remote sensing images refers to visible man-made objects in the images covering a variety of targets, such as ship, airplane, vehicle, etc. Although the majority of authors use the term 'ship detection' in their research, the expression 'sea target detection' or 'object recognition in ocean imagery' is also used to represent ship detection. All these terms will be deployed throughout this paper without an intended difference in meaning.

The remainder of this paper is organized as follows. In Section 2, chronological statistic on literatures of ship detection and classification methods is presented, and each procedure in the whole workflow is introduced. Typical methods in preprocess stage and detection and classification stage are systematically analyzed in Section 3. Besides, different levels in the classification stage are also narrated in this section. In Section 4, publicly available datasets are collected and introduced. Experimental results of some representative methods on one public dataset are provided and some issues in ship detection and classification are summarized in Section 5. Conclusions are drawn in Section 6.

## 2. Statistics

The analytical description in this paper is based on the collection of 153 papers (lists in Table A1 in the Appendix A) on ship detection and classification published from 1978 to July 2020, which describes the experimental results of their methods on optical satellite images. Comparative statistics and analysis between traditional feature-designed methods and the deep

Convolutional Neural Networks (CNN)<sup>10</sup> architecture based methods are introduced in this section, which is expected to lay the foundation for subsequent research.

### 2.1. Statistics on workflow of ship detection and classification

According to the statistics, the "Coarse-to-fine" two-stage detection scheme<sup>11,12</sup> is the classic processing framework on ship target detection for remote sensing images as shown in Fig. 1, which mainly includes three basic steps: image preprocessing, candidate target extraction, and target identification or classification. The one-stage detection scheme also applies in some methodologies, which completes the extraction of target candidates and identification or classification process in one step. (E.g. Refs.<sup>13–16</sup>) When the target is relatively large in the image to be detected, this scheme can obtain comparable efficiency with the two-stage detection scheme in the target detection task. However, in terms of time and computational saving, the two-stage detection scheme shows its superiority in treating wide-spread small target detection as in remote sensing images.<sup>11,12,17</sup> Therefore, the overview of existing detection algorithms in this section mainly focuses on the "Coarse-to-fine" two-stage detection scheme. The narrative of the one-stage scheme methodologies is placed in the process of target identification or classification in the following section. Some early literatures treat the term "ship classification" as the differentiation between real ship-targets and non-ships among ship candidates (E.g. Refs.<sup>6,11,18–20</sup>), which may cause misunderstanding of this term. To be clarifying, in this paper, the term "ship identification" denotes the distinction between ships and non-ships; the term "ship classification" indicates the distinction among different types of ship-targets.

#### (1) Image preprocessing

The most common processing in this step is the sea-land segmentation based on Geographic Information System (GIS) technology (E.g. Refs.<sup>21–26</sup>), because of the prior knowledge that large ships only appear in the marine area. The main advantages lay in this process are: firstly, reducing the computation time of feature extraction by narrowing traversal area of the core detection algorithm; secondly, improving detection precision by elimination of false detected targets caused by land part with complex texture features. Except for the sea-land segmentation process, the cloud filtering process is also applied in some ship detection and classification methods (E.g. Refs.<sup>4,25–28</sup>), aiming to provide reliable detection results in optical remote sensing images taken under cloudy and foggy weather conditions.

#### (2) Ship candidate extraction

Because the remote sensing image contains a vast sea area, the ship is relatively small and difficult to spot in the imaging result due to the image spatial resolution and the sparse distribution of targets.<sup>29,30</sup> If the dense feature extraction and calculation algorithms are directly executed in the entire sea area, the computational and time consumption will increase drastically. Therefore, most ship detection methods apply a "Coarse-to-fine" two-stage detection scheme. (E.g. Refs.<sup>11,12,19,21,31</sup>) Ship candidate extraction is the "coarse"

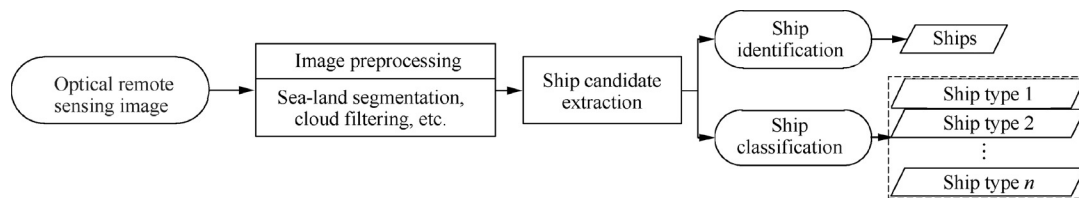


**Fig. 1** A common ship detection and classification workflow from optical remote sensing image.

stage, which utilizes a relatively simple computational feature descriptor to exclude most image regions without targets retaining possible target image blocks for further identification in the next step.

### (3) Ship identification and classification

The early published literature focuses its research purpose on ship identification because of the low spatial resolution of remote sensing imaging. (E.g. Refs. <sup>6,11,13,18–20,23,32</sup>) In the recent few decades, sophisticated ship classification methods emerge in response to the improvement in spatial resolution of the optical remote sensing imaging. (E.g. Refs. <sup>33–37</sup>) Therefore, ship identification and classification methods are introduced together in the following section. In this step, the common use of features such as shape, texture, and structure is to identify ships or the type of ship.

## 2.2. Statistics on methodologies of ship detection and classification

The CNN technology is applied in ship detection and classification of remote sensing image tasks increasingly since it demonstrates its powerful feature representation abilities in 2015.<sup>38</sup> For a better understanding, the term “CNN structure design based method” used in this paper refers to a method that focuses on designing and improving the CNN architecture for ship detection and classification; on the other hand, the term “feature design based method” refers to a method that focuses on designing feature descriptions for ships or backgrounds. Consequently, it provides statistical data on the number of publications, CNN structure design based methods, and feature design based methods in years respectively according to the literature collection mentioned above, as shown in Fig. 2. The feature design based methods dominant the early ship detection and classification research. However, ship detection and classification based on CNN structure design attract

majority research attention in recent years as the development of CNN technology.

The research boom of ship detection and classification appears in 2017 and then slightly downwards as can be seen in Fig. 2. This is the result of continuous improvement in the spatial resolution of optical remote sensing imaging. That improvement realizes imaging meaningful yet once unidentifiable targets such as airplanes and vehicles, which attract the attention of researchers. Ship target, thereby, is regarded as one of the categories of object detection from remote sensing images.

## 3. Analysis

In this section, the main application techniques in each step are demonstrated in accordance with the general process sequence for performing ship detection and classification.

### 3.1. Methodology for image preprocessing

In the procedure of image preprocessing, commonly used operations are sea-land segmentation, and cloud filtering, aiming at reducing the environmental influence during target detection procedure.

#### 3.1.1. Sea-land segmentation

Five basic methods lay in general utilized sea-land segmentation technology in ship detection and classification: (A) coastline matching method with the information stored in Geographic Information System (GIS); (B) regional homogeneity classification in the image; (C) methods based on the statistical model; (D) methods based on deep learning model; (E) methods based on normalized difference water index. Details of each basic method are narrated in the following.

#### (1) Coastline matching method

These methods mainly match the geographic location of the input image with that in GIS. The precision of its segmentation results only depends on the spatial resolution of the coastline stored in the GIS library and the accuracy of the imaging satellite positioning solution. It does not depend on the imaging quality, weather conditions or sensors. The disadvantage of these methods is that the geographic information of candidate areas is unavailable in some cases; besides, the available geographic coastline information may be outdated. The source of the coastline in GIS comes from the digital elevation model or digital terrain elevation data. The spatial resolution of the Shuttle Radar Topography Mission (SRTM) for global coverage is about 30 m, which achieves the highest possible

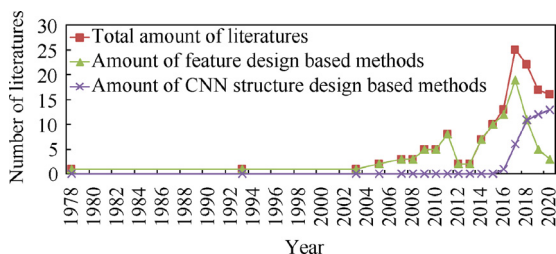


**Fig. 2** Literature collection statistics compiled from 1978 to May 2020.

resolution of global topographic data.<sup>39</sup> Although this spatial resolution of the coastline is sufficient to perform sea-land segmentation in satellite images of less than thirty meters resolution, it is far from the needs of sea-land segmentation in high spatial resolution satellite images.

## (2) Regional homogeneity classification

The initial step of the sea-land segmentation methods based on regional homogeneity classification is seed selection. Then the adjacent regions of the selected seed points are collected based on feature descriptors, and finally, the entire image is segmented.<sup>30</sup> Therefore, the seed selection is very vital in determining the segmentation results. Improper seed selection may lead to disastrous segmentation results. The segmentation results are also susceptible to weather conditions, sediment content in seawater, and sea surface reflections.

## (3) Methods based on statistical model

These methods establish statistical models based on the histogram of sea regions to approximate the intensity distribution of sea pixels and then determine the segmentation threshold of the sea area.<sup>40,41</sup> Sea-land segmentation based on these methods generally works well in most cases but will misclassify sea regions with abnormal intensity due to environmental factors. In most cases, these methods usually misclassify the land covered by cloud shadows as the sea.

## (4) Methods based on deep learning model

With the application of deep learning technology in the field of image segmentation, sea-land segmentation methods based on CNN technology have emerged in recent years.<sup>42–44</sup> In order to obtain a CNN based sea-land segmentation model, it is necessary to manually label the coastline samples at pixel-level on the image for the model training. The performance of these methods is relatively stable in resisting environmental factors in the image when performing segmentation. Comparing with methods based on statistical models or regional homogeneity classification, it obtains relatively higher precision in segmentation in most cases. However, it is easy to misclassify regions with complex contours and consume much more resources for computation and storage.

## (5) Methods based on normalized difference water index

To perform sea-land segmentation, these methods take advantage of the reflectance ratio from two different bands in the multispectral image to enhance the difference between sea and land.<sup>32,45</sup> However, the threshold applied to the ratio map for segmentation varies among different sensors. It needs to be adjusted when applied in images produced by other sensors. These methods are applicable to multispectral remote sensing images exclusively.

### 3.1.2. Cloud filtering

Optical remote sensing imaging is inevitably affected by weather conditions such as cloudy and foggy, which introduces interference within ship detection and classification and arouses false alarms.<sup>27</sup> Therefore, it is crucial to suppress the

influence of clouds and fog on optical remote sensing images when performing ship detection and classification tasks. There are three common methods in cloud filtering: (A) cloud mask threshold based on the Gaussian distribution model;<sup>4,25</sup> (B) threshold segmentation based on band ratio;<sup>26</sup> (C) cloud filter based on Fourier transform.<sup>27,28</sup>

There are two fundamental assumptions of the first method: the gray-scale values of the image follow the Gaussian distribution; cloud pixels mostly correspond to the brightest pixels in the images.<sup>4</sup> For thick cloud imaging in panchromatic images, most of their pixels reflect high intensity, but this is not always the case.

Band ratio between the NIR and B band is applied to perform threshold segmentation to eliminate clouds in multispectral images. The basic assumption behind it is that cloud pixels dominant to the top portion of the histogram.<sup>26</sup>

Cloud tends to extend spatially in low frequency component of the image, therefore, the center of the Fourier transform of the image containing the cloud raises sharply. Then the cloud filter is established by taking advantage of such feature to set the signal-to-noise ratio threshold.<sup>28</sup> However, it is easy to remove ships beneath the cloud in the process of cloud filtering.

### 3.2. Methodology for ship detection and classification

According to the statistics of literature collation in this paper, the following introduces ship detection and classification methods from two aspects: CNN structure design based methods and feature design based methods.

#### 3.2.1. Feature design based methodology

According to the statistics, ship detection and classification methods based on feature design generally adopt to the two-stage scheme, which includes ship candidate extraction and ship identification. There are basically two kinds of features in feature design based methodology, i.e., global feature and local feature. As shows in Fig. 3, a feature design based detector in two-stage manner usually applies both global feature and local feature combined with a discriminator; while a one-stage feature design based detector applies either global feature or local feature for discriminator. In ship candidate extraction stage, there mainly are six basic techniques: (A) threshold segmentation based on the statistical model; (B) background separation based on saliency; (C) anomaly detector; (D) background separation based on frequency analysis; (E) local feature descriptor on texture and shape, etc.; (F) background separation based on reflection difference. The main purpose at this stage is to quickly obtain the suspicious targets by separating the background and foreground with simple yet effective algorithms. Among them, (A)(B)(D)(F) belong to global feature; (E) belongs to local feature; (C) is a combination of global feature and local feature.

#### (1) Threshold segmentation based on statistical model

The statistical model derived by this technique generally bases on the difference of the gray-scale value between the ship and its local surroundings or the histogram of the gray-scale value of the whole image. Then, the statistical model distinguishes the background in the image by the threshold rule for-



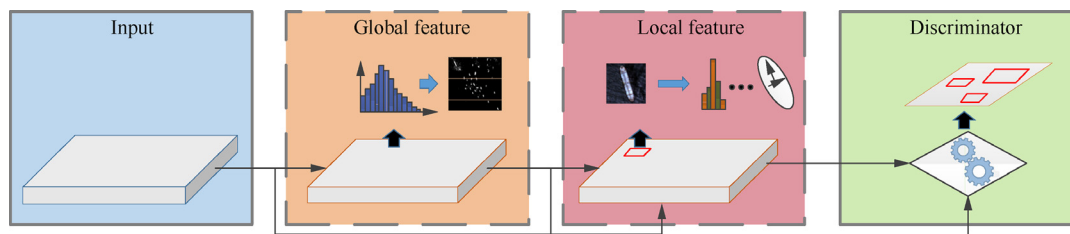


Fig. 3 Composition and workflow of a feature design based detector.

culated from the statistical data. (E.g. Refs.<sup>3,6,7,18,28,46–49</sup>) Methods based on simple numerical statistics achieve ideal results in simple scene background with little environmental changes. However, the environmental variation in optical remote sensing is uncontrollable due to the imaging mechanism. The statistical threshold rules are not always applicable in background segmentation in the images.

#### (2) Background separation based on saliency

The definition of “saliency” comes from the interpretation of the pre-attention mechanism in human visual search strategies,<sup>50</sup> which is applied to highlight salient signals and suppress backgrounds. (E.g. Refs.<sup>17,30,51–55</sup>) In order to measure the degree of saliency, Fourier transform (E.g. Refs.<sup>51–53</sup>) or histogram statistics (E.g. Refs.<sup>54</sup>), etc. is applied to the image to suppress the background, and thus the candidate target and the background are separated. It well performs in images with environmental noise caused by sea waves. The extraction results are unsatisfactory in images with messy sea surface containing small islands and cotton shaped clouds, as a consequence of that the highlighted signal may fall on these objects instead of real ship target.

#### (3) Anomaly detector

The essential idea of an anomaly detector is similar to the saliency mechanism. The occurrence of the targets in the image disobeys the background distribution rule in the original image, thus becomes an anomaly. (E.g. Refs.<sup>12,56–59</sup>) The detector is usually based on statistics and analysis of the sea surface without targets to obtain “normal” background distribution laws, and then selects the area with abnormal distribution as the candidate targets. Anomaly detector can maintain comparable performance under large-scale inference scenarios caused by ocean waves, clouds, or fog with that under calm sea background. However, it cannot adapt to complex backgrounds including various small-scale inferences.

#### (4) Background separation based on frequency analysis

Regarding the image as a two-dimensional discrete signal, the analysis based on its frequency domain believes that the noise and interference of waves and clouds can be effectively removed in this domain. (E.g. Refs.<sup>23,32,60–63</sup>) The commonly applied image frequency domain transformation is the Fourier transform and wavelet transform. Methods based on frequency analysis perform well when the disturbance has a relatively consistent pattern (such as ocean waves). They may fail

to detect such targets when two signals are superimposed, for example, ship occluded by mists.

#### (5) Local feature descriptor

These methods design detectors based on the observation of ship targets. They generalize the characteristics of ship targets’ texture, shape, and structure, etc. to formulate a feature descriptor for screening the ship. (E.g. Refs.<sup>64–69</sup>) These detectors can detect most of the ships, but the detection fails due to the low contrast between the ship and the surrounding environment. Moreover, numerous false targets are extracted by the detectors in the case of rich texture and edge information. Many feature descriptors used in optical remote sensing image ship candidate extraction mainly build on the histogram of oriented gradients and local binary patterns. (E.g. Refs.<sup>11,53,70–72</sup>)

#### (6) Background separation based on reflection difference

The principle of these methods is that the reflection intensity of the targets varies in different bands in remote sensing imaging. The ship candidates are extracted by using values from different bands to distinguish the reflection difference between the target and the background. (E.g. Refs.<sup>6,13,45,73,74</sup>) They take advantage of the imaging property, objects having different reflection intensity in multiple bands, to overcome the meteorological effects in optical remote sensing images. However, these methods neglect ships under the cloud shadows due to changes in the reflection intensity of these ships.

In the ship candidate extraction stage, many methods combine several of the above basic techniques to form a new model to achieve background separation under various meteorological conditions. (E.g. Refs.<sup>3,5,11,15,23,26,28,46,53–55,60,61,71,72,75,76</sup>).

In the ship identification and classification stage, feature design based methods mainly apply the strategy of combining classifiers and feature sets for discrimination. The frequently adopted classifier is the Support Vector Machine (SVM). The feature sets include (but not limited to) feature descriptors for ship geometric, shape, texture, and spectral signature.

#### 3.2.2. CNN structure design based methodology

After the CNN technique achieves remarkable results in object recognition and detection of natural scene images, it is gradually applied to the object detection task in remote sensing images. In order to obtain the CNN prediction model for object detection tasks, a large amount of labeled sample data is required for network training. During the training process, the sample data is fed forward into the network. Then the values of the convolution filters in the network are updated by

minimizing the loss function, which calculates the difference between the predicted values output by the current model and the ground truth of the labeled values. The update operation is achieved by the back propagating the error from the output layer of the network. This process stops when the loss function no longer shows a downward trend. After the training process, the parameters in each convolutional layer are fixed and saved for prediction. For the  $l$ -th convolutional layer, the unit  $j$  output  $y_j^l$  can be obtained from the unit  $i$  in previous layer  $y_i^{l-1}$  by<sup>77</sup>

$$y_j^l = g \left( \sum_{i \in S_j} y_i^{l-1} \otimes k_{ij}^l + b_j^l \right) \quad (1)$$

where  $S_j$  represents the collection of selected previous input maps,  $k_{ij}^l$  is the convolution filters between  $y_i^{l-1}$  and  $y_j^l$ ,  $b_j^l$  is the additive bias given by the current layer,  $\otimes$  denotes convolutional operation, and  $g(\cdot)$  is the activation function.

For a better understanding, we follow the illustration in Ref.<sup>78</sup> to unravel the components in the CNN model. As shows in Fig. 4, a CNN detector generally contains an input part, a backbone part, a head part may include a neck as an additional part. There are mainly two kinds of the CNN architectures, i.e., one-stage detector and two-stage detector. Their difference lies in whether to generate proposal regions as the intermediate result. The most representative one-stage detectors are Single Shot multibox Detector (SSD)<sup>79</sup> and You Only Look Once (YOLO),<sup>80,81</sup> which are frequently used in ship detection task from remote sensing images. As for the two stage detector, the most classic model is Faster R-CNN.<sup>82</sup> Due to the aerial view perspective in remote sensing imaging, the adjustment of architecture is necessary for the CNN model to predict targets with rotation variations. The usual adjustment is to add hidden layers for a specific purpose while maintaining the backbone structure of the networks. The CNN backbones commonly applied in ship detection and classification tasks are as follows (sorted according to the number of applications): ResNet<sup>38</sup> (E.g. Refs.<sup>31,83–97</sup>) and Visual Geometry Group (VGG)<sup>98</sup> (E.g. Refs.<sup>99–105</sup>). Usually Feature Pyramid Networks (FPN)<sup>106</sup> (E.g. Refs.<sup>85,88,97,102,107</sup>) or its modification version is used as the neck part. Faster R-CNN<sup>82</sup> (E.g. Refs.<sup>83,86–90,97,100,103,104,108,109</sup>), Mask R-CNN<sup>110</sup> (E.g. Refs.<sup>91,92,107,111</sup>), and Fast R-CNN<sup>112</sup> (E.g. Refs.<sup>105,113,114</sup>) are three general used sparse prediction detector heads; SSD<sup>79</sup> (E.g. Refs.<sup>99,101</sup>), and YOLO<sup>80,81</sup> (E.g. Refs.<sup>115,116</sup>) are two frequently applied dense prediction detector heads. In dealing with detection tasks in large-scale remote sensing images, these methods are far from meeting

real-time requirements after consuming numerous computational resources and storage space.

The convolutional filters obtained after the training process are believed to contain abstract object feature. However, the mechanism behinds the success of CNN is not revealed.

### 3.2.3. Ship classification

According to Refs.<sup>34,117,118</sup>, there are two levels in ship classification. In the first classification level, namely coarse-grained classification, ships are classified by some criteria into different categories. The second classification level refers to the fine-grained classification where ships are labeled by type, i.e., container ship, cargo ship etc.

In the coarse-grained classification, ships are conventionally divided into two categories, i.e., merchant ships or naval ships. (E.g. Refs.<sup>28,65</sup>) There are other coarse-grained classification criteria, e.g. Ref.<sup>119</sup> classifies ships into moving ships and static ships; Ref.<sup>120</sup> divide ships into four subclasses, namely fishing vessel, container vessel, sailing vessel and coast guard vessel; Ref.<sup>121</sup> classifies ships into multi, coast-ship and detail. Many coarse-grained classification methods conduct their experiment on BCCT200<sup>122,123</sup> dataset, which includes four classes, i.e., barge, cargo, container and tanker. (E.g. Refs.<sup>35–37,69,122–128</sup>) Except for Ref.<sup>129</sup> performs ship-fleets classification on satellite images at 10 m spatial resolution, other coarse-grained classification methods are implemented for images with a spatial resolution of more than 4 m. While the fine-grained classification methods are implemented on images with more than 2 m spatial resolution. (E.g. Refs.<sup>34,63,97,114,130–132</sup>)

The early proposed coarse-grained ship classification methods adopt a strategy of comparing the extracted ship features with a priori-database. (E.g. Refs.<sup>28,65</sup>) After the BCCT200 dataset is proposed, the most often used feature descriptor is multi-scale completed local binary pattern<sup>133</sup> combined with Gabor filter<sup>134</sup> to extract local and global features. (E.g. Refs.<sup>35,124,127</sup>) Methods for fine-grained ship classification generally apply CNN technique to identify ship types. (E.g. Refs.<sup>34,63,97,114,130</sup>) There are still few studies on coarse-grained and fine-grained ship classification. The main problem with ship classification may be that there is no uniform standard for data annotations for ship categories.

## 4. Publicly available datasets for ship detection and classification in remote sensing image

In recent years, many organizations release publicly available Earth observation datasets for object detection in the aerial

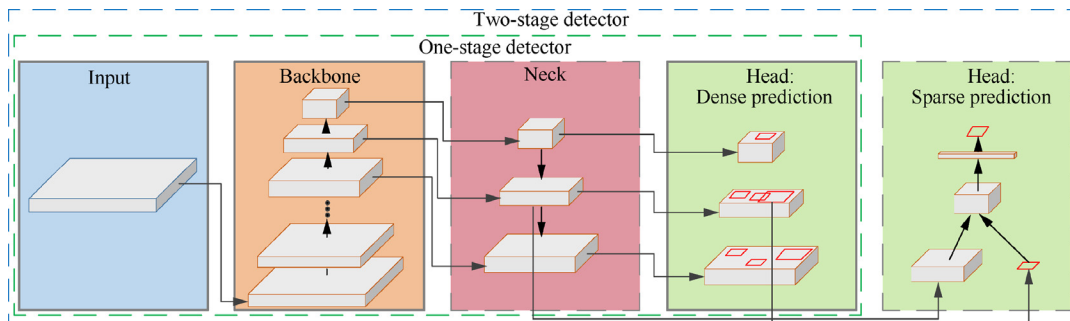


Fig. 4 Composition and workflow of ordinary CNN detector (partially source from Ref.<sup>78</sup>).

view. It provides researchers with a comparable platform to testify their algorithms.

There are nine datasets for ship detection and classification: (A) NWPU VHR-10, the earliest released dataset for evaluating the performance of object detection in remote sensing images<sup>135</sup>; (B) NWPU RESISC45 for scene classification in high-resolution optical satellite image data<sup>136</sup>; (C) HRSC2016, a dataset dedicated to ship detection and classification in high-resolution optical remote sensing images<sup>117</sup>; (D) Airbus Ship Detection dataset, from the challenge of ship detection on satellite images in Kaggle<sup>137</sup>; (E) xView, a dataset for object detection from satellite images<sup>138</sup>; (F) Dataset for Object detection in Aerial images (DOTA) dataset for object detection in aerial images<sup>139</sup>; (G) High-Resolution Remote Sensing object Detection (HRRSD) dataset for remote sensing image object detection applications<sup>140</sup>; (H) object Detection In Optical Remote sensing images (DOIR) dataset for object detection in optical remote sensing images<sup>141</sup>; (I) Fine-Grained Ship Detection (FGSD), the most detail labeled ship detection and classification dataset in remote sensing images so far (available soon).<sup>118</sup>

The NWPU VHR-10 dataset contains ten object classes: airplane, ship, storage tank, baseball diamond, tennis court, basketball court, ground track field, harbor, bridge, and vehicle.

NWPU RESISC45 dataset is a benchmark for scene classification in remote sensing images including 45 scene classes as follows: ship, airplane, airport, baseball diamond, basketball court, beach, bridge, chaparral, church, circular farmland, cloud, commercial area, dense residential, desert, forest, freeway, golf course, ground track field, harbor, industrial area, intersection, island, lake, meadow, medium residential, mobile home park, mountain, overpass, palace, parking lot, railway, railway station, rectangular farmland, river, roundabout, runway, sea ice, snowberg, sparse residential, stadium, storage tank, tennis court, terrace, thermal power station, and wetland.

The HRSC2016 dataset labels ship in three levels, namely ship class, ship category, and ship type. In the ship category level, it contains four labels: warcraft, aircraft carrier, merchant ship, and submarine. Note that, in this dataset, ships with unknown types are labeled with category level.

Airbus Ship Detection dataset contains the largest number of images in the dataset listed in this article. It reports in Ref.<sup>142</sup> that the combination of random forest classifier and feature sets containing the color histogram, Haralick textures and Hu moments outperforms the other four classifiers combined with the same feature sets, namely linear discriminant analysis, K-nearest neighbors, naïve bayes, and support vector machine.

The xView dataset contains 60 object categories and released by the Defense Innovation Unit Experimental (DIUx) and the National Geospatial-intelligence Agency (NGA). The 60 fine-grained classes are labeled in a parent class-child class manner. There are seven different parent classes, namely fixed-wing aircraft, passenger vehicle, truck, railway vehicle, maritime vessel, engineering vehicle, and building (some child classes have no parent class). In the maritime vessel class, it contains nine child classes: motoboat; sailboat; tugboat; barge; fishing vessel; ferry; yacht; container ship; oil tanker.

There are 15 classes in the DOTA dataset including plane, ship, storage tank, baseball diamond, tennis court, swimming

pool, ground track field, harbor, bridge, large vehicle, small vehicle, helicopter, roundabout, soccer ball field and basketball court.

In dataset HRRSD, there are 13 categories containing ship, airplane, baseball diamond, basketball court, bridge, cross-road, ground track field, harbor, parking lot, storage tank, T junction, tennis court, and vehicle.

The ship samples in FGSD are annotated not only the bounding boxes but also the rotated bounding boxes. It says there are 43 categories of ships in the dataset annotated in multi-level labels follow the same annotation manner as in HRSC2016 dataset. The category level contains labels of warship, carrier, submarine, and civil ship.

Table A2 in the Appendix A lists the detailed information of these datasets, including the acquisition source, resolution of images, image amount, and image size.

## 5. Discussion and future work

In this section, ship detection and coarse-grained classification results of mostly considered methods<sup>83,86,95,96,114,117,143,144</sup> on dataset HRSC2016 present in Table 1. The ship detection and classification tasks in HRSC2016 include three levels, i.e., L1, L2, and L3. L1 contains 1 class, namely ship; L2 contains 4 classes, i.e., Aircraft carrier (Air.), War craft (War.), Merchant ship (Mer.) and ship; L3 contains 19 classes, i.e., ship, Aircraft carrier, War craft, Merchant ship, Nimitz class aircraft carrier (Nim.), Enterprise class aircraft carrier (Ent.), Arleigh Burke class destroyer (Arl.), Whidbey Island class landing craft (Whi.), Perry class frigate (Per.), Sanantonio class amphibious transport dock (San.), Ticonderoga class cruiser (Tic.), Austen class amphibious transport dock (Aus.), Tarawa class amphibious assault ship (Tar.), Container ship (Con.), Command ship (Com.A), Car carrier A (Car.A), Container ship A (Con.A), Medical ship (Med.), Car carrier B (Car.B). Average precision (AP) and mean average precision<sup>145</sup> are used as the measurement criteria. The baseline method denotes to the BL2 algorithm in Ref.<sup>117</sup> and the RR-CNN refers to the RC1 algorithm in Ref.<sup>114</sup> in Table 1. It can be seen from Table 1 that RBox-CNN method achieves the best performance in both L1 and L2 tasks in HRSC2016 dataset. It yields a 91.9% AP value in L1 task and 79.4% mean AP in L2 task.

The L3 task performance of some representative methods on HRSC2016 displays in Table 2. The RC1 and RC2 algorithms both from Ref.<sup>114</sup>, where RC2 is basically the same as RC1 but adds a multi-task loss to learn non-maximum suppression score (Multi-NMS). The R-DFPN2 is based on R-DFPN and uses Proposals Simulation Generator (PSG) data augmentation in training process. Its input size is fixed at  $335 \times 58$  and is calculated by the k-means algorithm.<sup>97</sup> The results in Table 2 shows that the PSG data augmentation can improve the performance of the R-DFPN<sup>83</sup> in L3 task. Besides, the SHDRP<sup>97</sup> achieves the best preformation on L3 task of HRSC2016 so far and obtains 74.2% AP.

Based on the introduction and analysis of the literature collection on ship detection and classification from optical remote sensing images published in different periods, this chapter summarizes the main problems in these literatures as follows.

First, due to the passive remote sensing imaging characteristics of optical remote sensing images, the impact of environmental factors such as lighting and meteorological conditions

**Table 1** Comparisons of ship detection and classification methods on HRSC2016 (Source from Refs.<sup>86,95</sup>).

Methods	AP (%)					
	L1	L2				
		Air.	War.	Mer.	Ship	Mean
Baseline <sup>117</sup>	69.6	51.0	75.2	63.9	45.1	58.8
RR-CNN <sup>114</sup>	75.7	74.5	74.4	69.3	36.4	63.6
RRD <sup>144</sup>	84.3					
RBox-CNN <sup>86</sup>	91.9	95.1	93.1	77.5	51.9	79.4
R-DFPN <sup>83</sup>	79.6					
R-FCN <sup>96</sup>	82.3					
RoI Transformer <sup>145</sup>	86.2					
LAFCR <sup>95</sup>	90.3					

**Table 2** Comparisons of AP values on the L3 task of HRSC2016 (Source from Refs.<sup>97,114</sup>).

Class	AP (%)						
	Baseline <sup>117</sup>	RC1 <sup>114</sup>	RC2 <sup>114</sup> (RC1 + Multi-NMS)	Faster R-CNN <sup>82</sup>	R-DFPN <sup>83</sup>	R-DFPN2 <sup>83</sup> (R-DFPN + PSG <sup>97</sup> )	SHDRP <sup>97</sup>
Ship	41.9	34.3	32.9	45.6	46.7	36.8	<b>52.3</b>
War.	3.9	3.9	4.8	6.8	11.8	<b>33.4</b>	11.5
Car.A	53.1	61.0	56.7	72.7	55.5	70.8	<b>77.7</b>
Con.	36.8	56.2	40.2	42.1	42.1	58.4	<b>64.7</b>
Med.	78.8	<b>98.5</b>	62.5	0.0	34.5	90.9	95.5
San.	51.4	45.5	31.5	0.0	13.7	<b>95.0</b>	92.4
Whi.	50.9	51.8	45.8	20.9	20.4	75.4	<b>86.3</b>
Air.	41.2	53.9	40.3	18.9	30.8	72.3	<b>77.7</b>
Arl.	71.0	65.3	61.0	85.0	68.9	87.6	<b>91.3</b>
Car.B	67.8	67.8	57.6	51.6	65.0	94.5	<b>98.9</b>
Con.A	49.6	62.7	56.3	60.2	52.1	67.3	<b>72.8</b>
Nim.	44.6	59.3	65.0	64.6	68.0	<b>78.8</b>	67.2
Tar.	50.9	62.4	67.0	79.5	75.0	89.1	<b>96.5</b>
Mer.	12.8	27.4	18.2	<b>54.4</b>	22.0	10.0	17.9
Aus.	43.2	48.7	42.7	26.3	26.9	80.5	<b>86.3</b>
Com.A	57.1	50.5	38.4	17.0	33.2	85.2	<b>85.3</b>
Ent.	3.0	23.0	18.2	3.0	43.8	55.3	<b>55.7</b>
Per.	43.9	47.6	42.3	51.8	49.1	82.9	<b>91.9</b>
Tic.	57.4	48.6	49.8	69.4	66.6	84.2	<b>88.2</b>
Mean	45.2	51.0	43.7	40.5	43.5	71.0	<b>74.2</b>

during the imaging process reflects in the images, which has a great influence on the accuracy of ship detection. However, most of the methods collected in the literature collection cannot adapt to various environments. Among them, the relatively robust one is the detection methods taking advantage of the reflection signature of the target. Lacking the research in the analysis of the spectral reflection relationship between the target and background, none of these algorithms perform well under the influence of the target covered by cloud and shadow. Therefore, it is still a very challenging task that detects ships in remote sensing images under various environmental changes.

Second, as the remote sensing image covers a large area of the earth's surface, ship targets become relatively small and distribute sparsely on the image. In recent years, ship detection and classification methods based on CNN structure design become the mainstream applications. However, the neglected fact is that these methods require high-performance equipment and still cannot work efficiently. Efficiency has always been a

difficult problem in the object detection field, so there is no exception in ship detection from remote sensing images.

Third, the aerial view perspective in remote sensing images causes the target distortion according to the imaging angle of the satellite sensors and the relative position of the target. With the changes in scale and partial occlusion, the difficulty of the detection task enhances due to the variations of the targets' appearance and structure. Therefore, research on comprehensive features description on ship target and the utilization of imaging property in remote sensing to improve the detection accuracy is still ongoing.

Last but not the least, the problem in ship classification is the lack of a unified classification criterion among different datasets. Besides, affected by cloud cover or surrounding environment, the difference inner the ship classes may be greater than the difference between different ship classes. Few studies perform research on ship classification. And those methods have strict requirements on the completeness of ship extraction



as they based on the feature descriptor of shape, texture, and size of ships. Therefore, there is an urgent need to study ship classification in remote sensing images with the continuous improvement of spatial resolution.

All in all, there is still a gap between the current ship detection and classification technology and the practical application.

The upsurge of research on CNN technology leads to massive studies on object detection in optical remote sensing images applied such technique.<sup>141</sup> Although it makes great progress in object detection tasks in natural scene images, there still are a lot of rooms for improvement when performing in remote sensing images. Structure design that saves time and computational cost are very important in ship detection and classification from optical remotes sensing images.

With the number of publicly available dataset increases, the access for fine-grained labeled ship classes becomes convenient for researchers. These datasets provide a foundation for study on ship classification in aerial view images.

Unlike synthetic aperture radar, optical remote sensing images cannot resist weather conditions. It is an effective way to realize target detection to apply fusion information from different types of sensors.<sup>146</sup> Research on ship detection and classification based on multi-sourced information is promising in practical application.

## 6. Conclusions

In this paper, we provided statistics of 153 papers on ship detection and classification from 1978 to July 2020 and introduced

their commonly used detection scheme and workflow. In the image preprocessing procedure, sea-land segmentation and cloud filtering are introduced and the applied technologies in these two operations are analyzed. We classified the methods in these papers into two categories: the feature design based methods and the CNN structure design based methods. In the feature design based methods, six basic techniques were mainly adopted in the ship candidate extraction stage; the combination of classifiers with feature sets strategy was generally applied in the ship identification stage. In the CNN structure design based methods, designers usually made improvements in hidden layers while maintaining the backbone structure. There were two classic CNN backbone structures commonly applied in ship detection and classification from optical remote sensing images according to our literature collection. Finally, the detail information of nine public available datasets was listed, which can be applied to testify the ship detection and classification algorithms. Based on the analysis of the methods in these papers, we summarized the current problems and provided the possible future works on ship detection and classification methods for optical remote sensing images.

## Declaration of Competing Interest

The authors declare that they have no known competing financial interests or personal relationships that could have appeared to influence the work reported in this paper.

## Appendix A.

**Table A1** Literature collection of ship detection and classification methods published from 1978 to July 2020.(Literature collection from 1978 to 2016 partially source from Ref.<sup>147</sup>).

Year	Satellite sensor	Applied band	Resolution (m)		Minimum detection target (m)	Application purpose
			PAN	MS		
1978 <sup>45</sup>	Landsat-2 MSS	G,NIR	—	80	112	Ship detection
1993 <sup>32</sup>	SPOT XS	G,NIR	—	20	63	Ship detection
	Landsat TM	R,NIR	—	30	108	
2003 <sup>3</sup>	IKONOS	PAN,B,G,R,NIR	1	4	8	Ship detection
2005 <sup>64</sup>	SPOT-5	PAN	2.5	-	100	Ship detection
2005 <sup>148</sup>	IKONOS	PAN	1	-	10	Ship detection
	QuickBird		0.61	-		
2007 <sup>28</sup>	QuickBird	PAN	0.61	-	n/a	Ship detection and classification
2007 <sup>149</sup>	Google Earth	PAN	7	—	n/a	Ship detection
2007 <sup>150</sup>	IKONOS	PAN,NIR	1	4	2	Ship detection
2008 <sup>23</sup>	QuickBird	PAN	0.61	-	n/a	Ship detection
2008 <sup>25</sup>	SPOT-5	PAN	5	—	14	Ship detection and classification
2008 <sup>24</sup>	SPOT-5	PAN	5	—	n/a	Ship detection
2009 <sup>7</sup>	Landsat-7 ETM +	PAN,B,G,R,NIR,SWIR, MWIR,TIRS1,TIRS2	15	30	50	Ship detection
2009 <sup>151</sup>	QuickBird	n/a	-	2.5	n/a	Ship detection
2009 <sup>152</sup>	HJ-1	B	-	30	n/a	Ship detection
2009 <sup>65</sup>	VHR satellite images	B,G,R	-	1	n/a	Ship detection and calssification
2009 <sup>13</sup>	Landsat-5 TM	SWIR1,SWIR2	—	30	n/a	Ship detection

(continued on next page)

**Table A1** (continued)

Year	Satellite sensor	Applied band	Resolution (m)		Minimum detection target (m)	Application purpose
			PAN	MS		
2010 <sup>4</sup>	SPOT-5	PAN	5	—	20	Ship detection
2010 <sup>14</sup>	QuickBird	PAN	0.61	—	n/a	Ship detection
2010 <sup>15</sup>	Google Earth	B,G,R	n/a	n/a	150	Ship detection
2010 <sup>16</sup>	SPOT-5	PAN	5	—	15	Ship detection
2010 <sup>11</sup>	CBERS	G,R,NIR	—	20	n/a	Ship detection
	SPOT-2	PAN	10	—		
	SPOT-4		10			
	SPOT-5		5			
2011 <sup>5</sup>	MODIS	B,G,SWIR1,SWIR2,SWIR3	—	500	150	Ship detection
2011 <sup>153</sup>	SPOT-5	PAN	5	—	n/a	Ship detection
	QuickBird		0.61			
	Google Earth		10			
2011 <sup>46</sup>	SPOT-5	PAN	2.50	—	n/a	Ship detection
2011 <sup>154</sup>	Google Earth	B,G,R	—	0.5	10	Ship detection
2011 <sup>155</sup>	RapidEye	G	—	6.5	n/a	Ship detection
2011 <sup>18</sup>	GeoEye-1	PAN,B,G,R	0.41	1.65	n/a	Ship detection
2011 <sup>156</sup>	Google Earth	B,G,R	0.6	—	n/a	Ship detection
2011 <sup>122</sup>	Electro-Optical satellite	PAN	n/a	—	n/a	Ship classification
2012 <sup>123</sup>	Electro-Optical satellite	PAN	n/a	—	n/a	Ship classification
2012 <sup>17</sup>	SPOT-5	PAN	5	—	50	Ship detection
2012 <sup>52</sup>	Landsat-7 ETM +	B,G,R,NIR,SWIR1,SWIR2	30	—	n/a	Ship detection
2013 <sup>60</sup>	GeoEye-1	PAN,B,G,R,NIR	0.41	1.65	n/a	Ship detection
2013 <sup>26</sup>	WorldView-2	C,B,G,Y,R,RE,NIR1,NIR2	—	2.0	n/a	Ship detection
2014 <sup>47</sup>	GeoEye-1	B,G,R,NIR	0.41	1.65	4	Ship detection
	WorldView-2		0.5	2.0		
	IKONOS		1	4		
	QuickBird		0.61	2.5		
2014 <sup>66</sup>	QuickBird	PAN	0.61	—	n/a	Ship detection
2014 <sup>67</sup>	ASTER	G,R,NIR	—	15	15	Ship detection
2014 <sup>12</sup>	Google Earth	PAN	1	—	40	Ship detection
2014 <sup>68</sup>	Google Earth	PAN	0.5	—	n/a	Ship detection
2014 <sup>157</sup>	Google Earth	PAN	0.6	—	n/a	Ship detection
2014 <sup>56</sup>	SPOT-5	PAN	5	—	n/a	Ship detection
	Google Earth					
2015 <sup>69</sup>	IKONOS	PAN	1	—	n/a	Ship classification
	GeoEye-1		0.41			
	QuickBird		0.61			
	WorldView		0.5			
2015 <sup>158</sup>	Google Earth	PAN	≥4	—	n/a	Ship detection and classification
2015 <sup>27</sup>	GeoEye-1	PAN	0.41	—	n/a	Ship detection
2015 <sup>159</sup>	Google Earth	PAN	0.61	—	n/a	Ship detection
2015 <sup>61</sup>	GaoFen-1	PAN	2	—	n/a	Ship detection
2015 <sup>19</sup>	SPOT-5	PAN	5	—	50	Ship detection
2015 <sup>75</sup>	WorldView-2	PAN,B,G,R,NIR	0.5	1.8	n/a	Ship detection
	QuickBird-2		0.61	2.8		
	GeoEye-1		0.41	1.65		
	RapidEye		—	6.5		
	Formosat-2		2	8		
2015 <sup>160</sup>	Landsat-5 TM	SWIR2	—	30	n/a	Ship detection
	Landsat-7 ETM +					
2015 <sup>30</sup>	SPOT-5	PAN	0.5	—	n/a	Ship detection
2015 <sup>161</sup>	WorldView-2	PAN	0.5	—	n/a	Ship detection
2015 <sup>126</sup>	Electro-Optical satellite	PAN	n/a	—	n/a	Ship classification
2015 <sup>128</sup>	Electro-Optical satellite	PAN	n/a	—	n/a	Ship classification
2015 <sup>37</sup>	Electro-Optical satellite	PAN	n/a	—	n/a	Ship classification
2016 <sup>162</sup>	Sentinel-2	B,G,R,NIR	—	10	n/a	Ship detection
2016 <sup>163</sup>	Google Earth	B,G,R	—	0.12–0.25	n/a	Ship detection
2016 <sup>164</sup>	WorldView-1	PAN	0.5	—	n/a	Ship classification
	WorldView-2					
2016 <sup>165</sup>	Google Earth	B,G,R	—	0.4–2	n/a	Ship candidate extraction

**Table A1** (continued)

Year	Satellite sensor	Applied band	Resolution (m)		Minimum detection target (m)	Application purpose
			PAN	MS		
2016 <sup>20</sup>	Google Earth	PAN	—	1	n/a	Inshore ship detection
2016 <sup>166</sup>	WorldView-2	B,G,R,NIR	—	10	20	Ship detection
	QuickBird-2			(downsampled)		
	GeoEye-1					
2016 <sup>6</sup>	Sentinel-2	B,G,R,NIR	—	10	30	Ship motion detection
2016 <sup>167</sup>	Google Earth	n/a	—	—	n/a	Ship detection
2016 <sup>54</sup>	SkySat-1	PAN	1.1	—	n/a	Ship detection in video
2016 <sup>168</sup>	WorldView-1	PAN	0.5	—	25	Ship detection
2016 <sup>169</sup>	CBERS-02B	PAN	2.36	—	n/a	Ship detection
2016 <sup>170</sup>	Landsat-8	PAN, NIR,SWIR1,SWIR2, TIRS1,TIRS2	15	30	n/a	Ship detection
2016 <sup>171</sup>	WorldView-2	PAN,B,G,R,NIR	0.5	1.8	15	Ship detection
	QuickBird-2		0.61	2.8		
	GeoEye-1		0.41	1.65		
	RapidEye		—	6.5		
	Formosat-2		2	8		
	Sentinel-2		—	10		
2016 <sup>48</sup>	OrbView-3	PAN	1	—	n/a	Ship detection
2016 <sup>51</sup>	Google Earth	PAN	—	—	n/a	Ship detection
2016 <sup>21</sup>	GaoFen-1	PAN	2	—	10	Ship detection
	VRSS-1		2.5	—	320	
2017 <sup>57</sup>	VNREDSat-1	PAN	2.5	—	n/a	Ship detection
2017 <sup>73</sup>	GaoFen-1	PAN,B,G,R,NIR	2	8	n/a	Ship detection on inland rivers
2017 <sup>172</sup>	Google Earth	PAN	2	—	n/a	Ship detection
2017 <sup>55</sup>	Google Earth	B,G,R	—	—	n/a	Ship detection
2017 <sup>53</sup>	Google Earth	PAN	2	—	n/a	Ship detection
2017 <sup>173</sup>	Google Earth	B,G,R	—	1	n/a	Ship detection
2017 <sup>174</sup>	GaoFen-4	PAN,B,G,R,NIR	50	50	n/a	Ship motion detection
2017 <sup>175</sup>	Google Earth	PAN	—	2	n/a	Ship detection
2017 <sup>58</sup>	Google Earth	B,G,R	—	n/a	n/a	Ship detection
2017 <sup>176</sup>	Google Earth	B,G,R	—	1	n/a	Ship detection
2017 <sup>62</sup>	n/a	B,G,R	—	n/a	n/a	Ship detection
2017 <sup>31</sup>	GaoFen-2	B,G,R	—	4	100	Ship detection
2017 <sup>177</sup>	WorldView-2	PAN,B,G,R,NIR	0.5	1.8	20	Ship detection
2017 <sup>63</sup>	Google Earth	B,G,R	—	0.5	n/a	Ship detection and classification
2017 <sup>99</sup>	Google Earth	B,G,R	—	0.54	n/a	Ship detection
2017 <sup>178</sup>	Google Earth	B,G,R	—	2	n/a	Ship detection
2017 <sup>179</sup>	GaoFen-1	PAN	2	—	n/a	Sea-land-ship segmentation
2017 <sup>180</sup>	Google Map	B,G,R	—	1		
	RapidEye	B,G,R,RE,NIR	—	5	n/a	Ship detection and direction prediction
2017 <sup>131</sup>	QuickBird	PAN	0.61	—	n/a	Inshore ship detection and classification
2017 <sup>114</sup>	Google Earth	B,G,R	—	0.4–2	n/a	Ship detection and classification
2017 <sup>108</sup>	Google Earth	PAN	1	—	20	Ship detection
2017 <sup>130</sup>	Google Earth	B,G,R	—	0.5	n/a	Ship detection and classification
2017 <sup>49</sup>	Chinese agile remote sensing satellite	PAN	n/a	—	n/a	Ship detection in video
2017 <sup>74</sup>	Sentinel-2	B,G,R,NIR,SWIR1,SWIR2	—	10	n/a	Ship detection
2018 <sup>83</sup>	Google Earth	B,G,R	—	n/a	n/a	Ship detection
2018 <sup>181</sup>	Google Earth	B,G,R	—	1	n/a	Ship detection
2018 <sup>115</sup>	GaoFen-2	PAN	1	—	n/a	Ship detection
	Google Earth		0.3	—		
2018 <sup>182</sup>	Google Earth	PAN	n/a	—	2-30pixel	Ship detection
2018 <sup>183</sup>	CBERS-02B	PAN	2.36	—	n/a	Ship detection
	ZY3		2	—		
2018 <sup>119</sup>	GaoFen-2	PAN	0.81	—	n/a	Ship detection

(continued on next page)

**Table A1** (continued)

Year	Satellite sensor	Applied band	Resolution (m)		Minimum detection target (m)	Application purpose
			PAN	MS		
	WorldView-2		0.5			
	EROS-B		0.7			
2018 <sup>84</sup>	Google Earth	B,G,R	—	0.5	n/a	Ship detection and direction prediction
2018 <sup>85</sup>	Google Earth	B,G,R	—	1–5	n/a	Ship detection
2018 <sup>113</sup>	Google Earth	B,G,R	—	1	n/a	Ship detection
2018 <sup>101</sup>	Google Earth	B,G,R	—	0.2–1	n/a	Ship detection
2018 <sup>184</sup>	VNREDSat-1	B,G,R,NIR,PAN	2.5	2.5(pan-sharpened)	n/a	Ship candidate extraction
2018 <sup>127</sup>	Electro-Optical satellite	PAN	n/a	—	n/a	Ship classification
2018 <sup>185</sup>	GaoFen-4	B,G,R,NIR,PAN	50	50	2 pixel	Ship tracking
2018 <sup>124</sup>	Electro-Optical satellite	PAN	n/a	—	n/a	Ship classification
2018 <sup>100</sup>	Google Earth	B,G,R	—	0.4–2	n/a	Ship detection
2018 <sup>121</sup>	Microsoft Bing maps	B,G,R	—	n/a	4 pixels	Ship detection and classification
2018 <sup>125</sup>	Electro-Optical satellite	PAN	n/a	—	n/a	Ship classification
2018 <sup>96</sup>	Google Earth	B,G,R	—	1	n/a	Ship detection
2018 <sup>71</sup>	SPOT-5	PAN	5	—	n/a	Ship detection
	GaoFen-1		2			
2018 <sup>186</sup>	JiLin-1	B,G,R	—	0.72	n/a	Ship detection
	Google Earth			1		
2018 <sup>86</sup>	Google Earth	B,G,R	—	0.4–2	n/a	Ship detection and classification
2018 <sup>87</sup>	Google Earth	B,G,R	—	1	8 pixel width, 11 pixel length	Ship detection
2019 <sup>88</sup>	GaoFen-1	PAN	2	—	n/a	Ship detection
	GaoFen-2		0.81			
	JiLin-1		0.72			
2019 <sup>120</sup>	n/a	PAN	2.6	—	n/a	Ship detection and classification
2019 <sup>59</sup>	GaoFen-1	PAN	2	—	n/a	Ship detection
	GaoFen-2		0.81			
2019 <sup>109</sup>	GaoFen-2	B,G,R,NIR,PAN	1	1(pan-sharpened)	n/a	Ship detection
2019 <sup>187</sup>	Sentinel-2	B,G,R,NIR	—	10	20	Ship detection
	SWIR			20		
2019 <sup>35</sup>	Electro-Optical satellite	PAN	n/a	—	n/a	Ship classification
2019 <sup>89</sup>	Google Earth	B,G,R	—	3	n/a	Ship detection
2019 <sup>29</sup>	Google Earth	B,G,R	—	n/a	n/a	Ship candidate extraction
2019 <sup>129</sup>	Sentinel-2	B,G,R,NIR	—	10	n/a	Ship detection and classification
2019 <sup>90</sup>	n/a	PAN	0.2–3	—	n/a	Ship detection
2019 <sup>36</sup>	Electro-Optical satellite	PAN	n/a	—	n/a	Ship classification
2019 <sup>97</sup>	Google Earth	B,G,R	—	0.4–2	n/a	Ship detection and classification
	QuickBird	PAN	0.61	—		
2019 <sup>132</sup>	Google Earth	B,G,R	—	0.4–2	n/a	Ship classification
2019 <sup>188</sup>	GO-3S	PAN	n/a	—	n/a	Ship detection in video
2019 <sup>107</sup>	Google Earth	B,G,R	—	0.4–2	n/a	Ship detection
2019 <sup>189</sup>	Google Earth	B,G,R	—	0.5	n/a	Ship detection
2019 <sup>111</sup>	SPOT-6	PAN, B,G,R,NIR	1.5	6	22	Ship detection
2019 <sup>91</sup>	Google Earth	B,G,R	—	0.4–2	n/a	Ship detection
2019 <sup>190</sup>	n/a*	B,G,R	—	n/a	n/a	Ship detection
2020 <sup>92</sup>	n/a*	B,G,R	—	n/a	n/a	Ship detection
2020 <sup>95</sup>	Google Earth	B,G,R	—	n/a	n/a	Ship detection
2020 <sup>34</sup>	Google Earth	B,G,R	—	0.4–2	n/a	Ship classification
	GaoFen-1	PAN	2	—		
2020 <sup>72</sup>	GaoFen-2	PAN	0.81	—	n/a	Ship detection
	ZY-3		2.1			
2020 <sup>102</sup>	Google Earth	B,G,R	—	0.5	20 × 20	Ship detection
2020 <sup>103</sup>	Google Earth	B,G,R	—	1	80	Ship detection



**Table A1** (continued)

Year	Satellite sensor	Applied band	Resolution (m)		Minimum detection target (m)	Application purpose
			PAN	MS		
2020 <sup>33</sup>	n/a	B,G,R	—	n/a	n/a	Ship detection and classification
2020 <sup>191</sup>	Google Earth	B,G,R	—	0.4–2	Average 150 pixels	Ship detection
2020 <sup>192</sup>	Google Earth	PAN	n/a	—	n/a	Ship detection and classification
2020 <sup>93</sup>	Google Earth	B,G,R	—	0.2–30	n/a	Ship detection and segmentation
2020 <sup>104</sup>	Google Earth	B,G,R	—	0.4–2	n/a	Ship detection
2020 <sup>193</sup>	n/a	B,G,R	—	n/a	n/a	Ship detection
2020 <sup>22</sup>	GaoFen-1	B,G,R,NIR	—	8	80	Ship detection
	SJ9			10	50	
	ZY3			6	30	
	CB04			20	100	
2020 <sup>94</sup>	Google Earth	B,G,R	—	n/a	n/a	Ship detection
	JiLin-1			≤2.88		
	GaoFen-2			3.2		
2020 <sup>116</sup>	Google Earth	B,G,R	—	0.27–2.15	n/a	Ship detection
2020 <sup>105</sup>	Google Earth	B,G,R	—	n/a	n/a	Ship detection
2020 <sup>194</sup>	Google Earth	B,G,R	—	1–5	n/a	Ship detection
	GaoFen-2		—	3.2		
2020 <sup>76</sup>	Google Earth	B,G,R	—	0.4–2	n/a	Ship detection
	JiLin-1			≤2.88		
	GaoFen-2			3.2		

\* Performed on Airbus Ship Detection dataset.

**Table A2** Detail information of datasets that can be applied to ship detection.

Dataset abbreviation	Resolution (m)	Image source	Image amount	Application purpose	Image size (pixel)
NWPU VHR-10	0.5–2 0.08	Google Earth Vaihingen dataset <sup>195</sup>	715 85	Object classification	956 × 554–1073 × 704
NWPU-RESISC45	0.2–30	Google Earth	31,500 (700 each class)	Scene classification	256 × 256
HRSC 2016	0.4–2	Google Earth	1061	Ship detection and classification	300 × 300–1500 × 900
Airbus Ship Detection	n/a	n/a	208,162	Ship detection	768 × 768
xView	0.3	WorldView-3	1413	Object classification	2772 × 2678–5121 × 3023
DOTA v1.5	n/a ≤2.88 3.2	Google Earth JiLin-1 GaoFen-2	2806	Object classification	800 × 800–4000 × 4000
HRRSD	0.15–1.2 0.6–1.2	Google Earth Baidu Map	21,761 4961	Object classification	493 × 402–2077 × 2606
DIOR	0.5–30	Google Earth	23,463	Object classification	800 × 800
FGSD	0.12–1.93	Google Earth	4736	Ship detection and classification	930 × 930

## References

- Xu C, Wang Y, Ai W. Situation assessment in the warships-airplanes joint operation based on parameter learning in Bayesian network *Proceedings of IEEE chinese guidance, navigation and control conference; 2014 Aug 8–10; Yantai. China*. Piscataway: IEEE Press; 2014. p. 2014.
- Riveiro M, Falkman G, Ziemke T. Improving maritime anomaly detection and situation awareness through interactive visualization *11th international conference on information fusion; 2008 Jun 30–Jul 3; Cologne. Germany*. Piscataway: IEEE Press; 2008. p. 2008.
- Pegler KH, Coleman DJ, Zhang Y, et al. The potential for using very high spatial resolution imagery for marine search and rescue surveillance. *Geocarto International* 2003;**18**(3):35–9.

4. Corbane C, Najman L, Pecoul E, et al. A complete processing chain for ship detection using optical satellite imagery. *International Journal of Remote Sensing* 2010;**31**(22):5837–54.
5. Dorado-Muñoz LP, Velez-Reyes M. Ship detection in MODIS imagery *Proceedings of SPIE 8048, algorithms and technologies for multispectral, hyperspectral, and ultraspectral imagery XVII, SPIE defense, security, and sensing*; 2011 May 20; Orlando, USA. Bellingham: SPIE; 2011. p. 2011.
6. Heiselberg H. A direct and fast methodology for ship recognition in Sentinel-2 multispectral imagery. *Remote Sensing* 2016;**8**(12):1033.
7. Abileah R. Surveying coastal ship traffic with LANDSAT. *OCEANS 2009; 2009 Oct 26-29; Biloxi, USA*. Piscataway: IEEE Press; 2009.
8. Stennis carrier strike group exits south china sea days after arriving [Internet]. [updated 2016 Mar 8; cited 2020 Jun 11]. Available from: < <https://www.military.com/daily-news/2016/03/08/stennis-carrier-strike-group-exits-south-china-sea-days-arriving.html> > .
9. Goetz AF, Vane G, Solomon JE, et al. Imaging spectrometry for Earth remote sensing. *Science* 1985;**228**(4704):1147–53.
10. Krizhevsky A, Sutskever I, Hinton GE. ImageNet classification with deep convolutional neural networks *International conference on neural information processing systems*; 2012 Dec 3-6; Lake Tahoe, USA. New York: ACM; 2012. p. 2012.
11. Zhu C, Zhou H, Wang R, et al. A novel hierarchical method of ship detection from spaceborne optical image based on shape and texture features. *IEEE Transactions on Geoscience and Remote Sensing* 2010;**48**(9):3446–56.
12. Shi Z, Yu X, Jiang Z, et al. Ship detection in high-resolution optical imagery based on anomaly detector and local shape feature. *IEEE Transactions on Geoscience and Remote Sensing* 2014;**52**(8):4511–23.
13. Wu G, de Leeuw J, Skidmore AK, et al. Performance of landsat TM in ship detection in turbid waters. *International Journal of Applied Earth Observation and Geoinformation* 2009;**11**(1):54–61.
14. Harvey N, Porter R, Theiler J. Ship detection in satellite imagery using rank-order grayscale hit-or-miss transforms. *Proceedings of SPIE 7701, visual information processing XIX, SPIE defense, security, and sensing*; 2010 Apr 15; Orlando, USA. Bellingham: SPIE; 2010.
15. Ma L, Guo J, Wang Y, et al. Ship detection by salient convex boundaries. *2010 3rd international congress on image and signal processing*; 2010 Oct 16-18; Yantai, China. Piscataway: IEEE Press; 2010.
16. Proia N, Pagé V. Characterization of a bayesian ship detection method in optical satellite images. *IEEE Geoscience and Remote Sensing Letters* 2010;**7**(2):226–30.
17. Bi F, Zhu B, Gao L, et al. A visual search inspired computational model for ship detection in optical satellite images. *IEEE Geoscience and Remote Sensing Letters* 2012;**9**(4):749–53.
18. Wu W, Luo J, Qiao C, et al. Ship recognition from high resolution remote sensing imagery aided by spatial relationship. *Proceedings 2011 IEEE international conference on spatial data mining and geographical knowledge services*; 2011 Jun 29-Jul 1; Fuzhou, China. Piscataway: IEEE Press; 2011.
19. Tang J, Deng C, Huang G-B, et al. Compressed-domain ship detection on spaceborne optical image using deep neural network and extreme learning machine. *IEEE Transactions on Geoscience and Remote Sensing* 2015;**53**(3):1174–85.
20. Li S, Zhou Z, Wang B, et al. A novel inshore ship detection via ship head classification and body boundary determination. *IEEE Geoscience and Remote Sensing Letters* 2016;**13**(12):1920–4.
21. Zou Z, Shi Z. Ship detection in spaceborne optical image with SVD networks. *IEEE Transactions on Geoscience and Remote Sensing* 2016;**54**(10):5832–45.
22. Xie X, Li B, Wei X. Ship selection in multispectral satellite images under complex environment. *Remote Sensing* 2020;**12**(5):792.
23. Buck H, Sharghi E, Guilas C, et al. Enhanced ship detection from overhead imagery. *Proceedings of SPIE 6945, optics and photonics in global homeland security IV, SPIE defense and security symposium*; 2008 Apr 15; Orlando, USA. Bellingham: SPIE; 2008.
24. Corbane C, Petit M. Fully automated procedure for ship detection using optical satellite imagery. *Proceedings of SPIE 7150, remote sensing of inland, coastal, and oceanic waters, SPIE asia-pacific remote sensing*; 2008 Dec 19; Noumea, New Caledonia. Bellingham: SPIE; 2008.
25. Corbane C, Marre F, Petit M. Using SPOT-5 HRG data in panchromatic mode for operational detection of small ships in tropical area. *Sensors* 2008;**8**(5):2959–73.
26. Daniel B, Schaum A, Allman E, et al. Automatic ship detection from commercial multispectral satellite imagery. *Proceedings of SPIE 9817, algorithms and technologies for multispectral, hyperspectral, and ultraspectral imagery XIX, SPIE defense, security, and sensing*; 2013 May 18; Baltimore, USA. Bellingham: SPIE; 2013.
27. Jin T, Zhang J. Ship detection from high-resolution imagery based on land masking and cloud filtering. *Proceedings of SPIE 9817, seventh international conference on graphic and image processing*; 2015 Dec 9; Singapore. Bellingham: SPIE; 2015.
28. Buck H, Sharghi E, Bromley K, et al. Ship detection and classification from overhead imagery. *Proceedings of SPIE 6696, Applications of digital image processing XXX, optical engineering + applications*; 2007 Sep 24; San Diego, USA. Bellingham: SPIE; 2007.
29. Tan Y, Liang H, Guan Z, et al. Visual saliency based ship extraction using improved bing. *IGARSS 2019 - 2019 IEEE international geoscience and remote sensing symposium*; 2019 Jul 28-Aug 2; Yokohama, Japan. Piscataway: IEEE Press; 2019.
30. Yang F, Xu Q, Gao F, et al. Ship detection from optical satellite images based on visual search mechanism. *2015 IEEE International Geoscience and Remote Sensing Symposium (IGARSS)*; 2015 Jul 26-31; Milan, Italy. Piscataway: IEEE Press; 2015.
31. Lin H, Shi Z, Zou Z. Fully convolutional network with task partitioning for inshore ship detection in optical remote sensing images. *IEEE Geoscience and Remote Sensing Letters* 2017;**14**(10):1665–9.
32. Burgess DW. Automatic ship detection in satellite multispectral imagery. *Photogrammetric Engineering and Remote Sensing* 1993;**59**(2):229–37.
33. Jia H, Ni L. Marine ship recognition based on cascade CNNs. *Proceedings of SPIE 11427, second target recognition and artificial intelligence summit forum*; 2020 Jan 31; Changchun, China. Bellingham: SPIE; 2020.
34. Zhang X, Lv Y, Yao L, et al. A new benchmark and an attribute-guided multilevel feature representation network for fine-grained ship classification in optical remote sensing images. *IEEE Journal of Selected Topics in Applied Earth Observations and Remote Sensing* 2020;**13**:1271–85.
35. Shi Q, Li W, Tao R, et al. Ship classification based on multifeature ensemble with convolutional neural network. *Remote Sensing* 2019;**11**(4):419.
36. Hilton C, Parameswaran S, Dotter M, et al. Classification of maritime vessels using capsule networks. *Proceedings of SPIE 10992, geospatial informatics IX, SPIE defense + commercial sensing*; 2019 Jun 18; Baltimore, USA. Bellingham: SPIE; 2019.
37. Verbanacs P, Harguess J. Feature Learning HyperNEAT: evolving neural networks to extract features for classification of maritime satellite imagery. In: Lones M, Tyrrell A, Smith S, editors. *Information Processing in Cells and Tissues. IPCAT 2015: Information processing in cells and tissues*; 2015 Sep 14-16; San Diego, USA. Cham: Springer International Publishing; 2015.
38. He K, Zhang X, Ren S, et al. Deep residual learning for image recognition. *2016 IEEE conference on Computer Vision and*

- Pattern Recognition(CVPR)*; 2016 Jun 27-30; Las Vegas, USA. Piscataway: IEEE Press; 2016.
39. Roth A, Marschall U, Knöpfle W, et al. SRTM- X-SAR products and quality. EUSAR 2000; 2000 May 23-25; München, Germany; 2000.
  40. You X, Li W. A sea-land segmentation scheme based on statistical model of sea. *2011 4th international congress on image and signal processing*; 2011 Oct 15-17; Shanghai, China. Piscataway: IEEE Press; 2011.
  41. Jubelin G, Khenchaf A. A statistical model of sea clutter in panchromatic high resolution images. *2012 IEEE international geoscience and remote sensing symposium*; 2012 Jul 22-27; Munich, Germany. Piscataway: IEEE Press; 2012.
  42. Miao Z, Fu K, Sun H, et al. Automatic water-body segmentation from high-resolution satellite images via deep networks. *IEEE Geoscience and Remote Sensing Letters* 2018;**99**:1–5.
  43. Li R, Liu W, Yang L, et al. DeepUNet: a deep fully convolutional network for pixel-level sea-land segmentation. *IEEE Journal of Selected Topics in Applied Earth Observations and Remote Sensing* 2018;**11**(11):3954–62.
  44. Cheng D, Meng G, Cheng G, et al. SeNet: structured edge network for sea-land segmentation. *IEEE Geoscience and Remote Sensing Letters* 2016;**99**:1–5.
  45. McDonnell MJ, Lewis AJ. Ship detection from LANDSAT. *Photogrammetric Engineering and Remote Sensing* 1978;**44** (3):297–301.
  46. Huang G, Wang Y, Zhang Y, et al. Ship detection using texture statistics from optical satellite images. *2011 international conference on digital image computing: Techniques and applications*; 2011 Dec 6-8; Noosa, Australia. Piscataway: IEEE Press; 2011.
  47. Kanjir U, Marsetić A, Pehani P, et al. An automatic procedure for small vessel detection from very-high resolution optical imagery. *Proceedings of the 5th GEOBIA*; 2014 May 21-24; Thessaloniki, Greece, 2014.
  48. Xie X, Xu Q, Hu L. Fast ship detection from optical satellite images based on ship distribution probability analysis. *2016 4th international workshop on Earth Observation and Remote Sensing Applications (EORS)*; 2016 Jul 4-6; Guangzhou, China. Piscataway: IEEE Press; 2016.
  49. Yao S, Chang X, Cheng Y, et al. Detection of moving ships in sequences of remote sensing images. *ISPRS International Journal of Geo-Information* 2017;**6**(11):334.
  50. Itti L, Koch C, Niebur E. A model of saliency-based visual attention for rapid scene analysis. *IEEE Transactions on Pattern Analysis and Machine Intelligence* 1998;**20**(11):1254–9.
  51. Xu F, Liu J-H. Ship detection and extraction using visual saliency and histogram of oriented gradient. *Optoelectronics Letters* 2016;**12**(6):473–7.
  52. Ding Z, Yu Y, Wang B, et al. An approach for visual attention based on biquaternion and its application for ship detection in multispectral imagery. *Neurocomputing* 2012;**76**(1):9–17.
  53. Yang F, Xu Q, Li B. Ship detection from optical satellite images based on saliency segmentation and structure-LBP feature. *IEEE Geoscience and Remote Sensing Letters* 2017;**14** (5):602–6.
  54. Li H, Man Y. Moving ship detection based on visual saliency for video satellite. *2016 IEEE International Geoscience and Remote Sensing Symposium (IGARSS)*; 2016 Jul 10-15; Beijing, China. Piscataway: IEEE Press; 2016.
  55. Xu F, Liu J, Sun M, et al. A hierarchical maritime target detection method for optical remote sensing imagery. *Remote Sensing* 2017;**9**(3):280.
  56. Yang G, Li B, Ji S, et al. Ship detection from optical satellite images based on sea surface analysis. *IEEE Geoscience and Remote Sensing Letters* 2014;**11**(3):641–5.
  57. Lư Việt H. Operational detection and management of ships in vietnam coastal region using Vnedsat-1 image [dissertation]. Vietnam: Vietnam National University; 2017.
  58. Shao X, Li H, Lin H, et al. Ship detection in optical satellite image based on RX method and PCANet. *Sensing and Imaging* 2017;**18**(1):21.
  59. Wang N, Li B, Xu Q, et al. Automatic ship detection in optical remote sensing images based on anomaly detection and SPP-PCANet. *Remote Sensing* 2019;**11**(1):47.
  60. Bouma H, Dekker R, Schoemaker R, et al. Segmentation and wake removal of seafaring vessels in optical satellite images. *Proceedings of SPIE 8897, electro-optical remote sensing, photonic technologies, and applications VII; and military applications in hyperspectral imaging and high spatial resolution sensing, SPIE security + defence*; 2013 Oct 15; Dresden, Germany. Bellingham: SPIE; 2013.
  61. Shengxiang Q, Jie M, Jin L, et al. Unsupervised ship detection based on saliency and S-HOG descriptor from optical satellite images. *IEEE Geoscience and Remote Sensing Letters* 2015;**12** (7):1451–5.
  62. Huang B, Xu T, Chen S, et al. A novel algorithm based on wavelet transform for ship target detection in optical remote sensing images. *Proceedings of SPIE 10420, ninth International Conference on Digital Image Processing (ICDIP 2017)*; 2017 Jul 21; Hong Kong, China. Bellingham: SPIE; 2017.
  63. Liu Y, Cui H-Y, Kuang Z, et al. Ship detection and classification on optical remote sensing images using deep learning *ITM Web of Conferences*. p. 05012.
  64. Wang M, Luo J, Zhou C, et al. A shape constraints based method to recognize ship objects from high spatial resolution remote sensed imagery. In: Sunderam VS, Van Albada GD, Sloot PMA, editors. *Computational Science. ICCS 2005: Computational Science-ICCS 2005*; 2005 May 22-25; Atlanta, USA. Berlin, Heidelberg: Springer Berlin Heidelberg; 2005.
  65. Tao C, Tan Y, Cai H, et al. Ship detection and classification in high-resolution remote sensing imagery using shape-driven segmentation method. *Proceedings of SPIE 7495, MIPPR 2009: Automatic target recognition and image analysis, sixth international symposium on multispectral image processing and pattern recognition*; 2009 Oct 30; Yichang, China. Bellingham: SPIE; 2009.
  66. Liu G, Zhang Y, Zheng X, et al. A new method on inshore ship detection in high-resolution satellite images using shape and context information. *IEEE Geoscience and Remote Sensing Letters* 2014;**11**(3):617–21.
  67. Partsinevelos P, Miliareis G, Tripolitsiotis A. Ship extraction and categorization from ASTER VNIR imagery. *Proceedings of SPIE 9229, second international conference on Remote Sensing and Geoinformation of the Environment (RSCy2014)*; 2014 Aug 12; Paphos, Cyprus. Bellingham: SPIE; 2014.
  68. Xia Y, Wan S, Jin P, et al. A novel sea-land segmentation algorithm based on local binary patterns for ship detection. *International Journal of Signal Processing, Image Processing and Pattern Recognition* 2014;**7**(3):237–46.
  69. Arguedas VF. Texture-based vessel classifier for electro-optical satellite imagery. *2015 IEEE International Conference on Image Processing (ICIP)*; 2015 Sep 27-30; Quebec City, Canada. Piscataway: IEEE Press; 2015.
  70. Dong C, Liu J, Xu F, et al. Ship detection from optical remote sensing images using multi-scale analysis and fourier HOG descriptor. *Remote Sensing* 2019;**11**(13):1529.
  71. Zhuang Y, Qi B, Chen H, et al. Locally oriented scene complexity analysis real-time ocean ship detection from optical remote sensing images. *Sensors* 2018;**18**(11):3799.
  72. Nie T, Han X, He B, et al. Ship detection in panchromatic optical remote sensing images based on visual saliency and multi-dimensional feature description. *Remote Sensing* 2020;**12** (1):152.
  73. Liu B, Li Y, Zhang Q, et al. The application of GF-1 imagery to detect ships on the yangtze river. *Journal of the Indian Society of Remote Sensing* 2017;**45**(1):179–83.

74. Heiselberg P, Heiselberg H. Ship-iceberg discrimination in Sentinel-2 multispectral imagery by supervised classification. *Remote Sensing* 2017;9(11):1156.
75. Topputo F, Massari M, Lombardi R, et al. Space shepherd: Search and rescue of illegal immigrants in the mediterranean sea through satellite imagery. *2015 IEEE International Geoscience and Remote Sensing Symposium (IGARSS)*; 2015 Jul 26-31; Milan, Italy.. Piscataway: IEEE Press; 2015.
76. Zhuang Y, Lianlin L, He C. Small sample set inshore ship detection from VHR optical remote sensing images based on structured sparse representation. *IEEE Journal of Selected Topics in Applied Earth Observations and Remote Sensing* 2020;13:2145–60.
77. Bouvrie J. Notes on convolutional neural networks. Boston: Massachusetts Institute of Technology; 2006.
78. Bochkovskiy A, Wang C, Liao H. YOLOv4: Optimal speed and accuracy of object detection [Internet] [updated 2020 Apr 23; cited 2020 Jun 11] Available from: 2020; <<https://arxiv.org/abs/2004.10934>> .
79. Liu W, Anguelov D, Erhan D, et al. SSD: single shot MultiBox detector. Berlin: Springer; 2016.
80. Redmon J, Farhadi A. YOLO9000: better, faster, stronger. *2017 IEEE conference on Computer Vision and Pattern Recognition (CVPR)*; 2017 Jul 21-26; Honolulu, USA. Piscataway: IEEE Press; 2017.
81. Redmon J, Farhadi A. Yolov3: An incremental improvement [Internet] [updated 2020 Apr 23; cited 2020 Jun 11] Available from: <<https://arxiv.org/abs/1804.02767>> .
82. Ren S, He K, Girshick R, et al. Faster R-CNN: towards real-time object detection with region proposal networks. *IEEE Transactions on Pattern Analysis and Machine Intelligence* 2017;39(6):1137–49.
83. Yang X, Sun H, Fu K, et al. Automatic ship detection in remote sensing images from Google Earth of complex scenes based on multiscale rotation dense feature pyramid networks. *Remote Sensing* 2018;10(1):132.
84. Yang X, Sun H, Sun X, et al. Position detection and direction prediction for arbitrary-oriented ships via multitask rotation region convolutional neural network. *IEEE Access* 2018;6:50839–49.
85. Wang Y, Li W, Li X, et al. Ship detection by modified retinanet. *2018 10th IAPR workshop on Pattern Recognition in Remote Sensing (PRRS)*; 2018 Aug 19-20; Beijing, China. Piscataway: IEEE Press; 2018.
86. Koo J, Seo J, Jeon S, et al. RBox-CNN: Rotated bounding box based CNN for ship detection in remote sensing image. *Proceedings of the 26th ACM SIGSPATIAL international conference on advances in geographic information systems*; 2018 Nov; Seattle, Washington, USA. New York: ACM; 2018.
87. Fu K, Li Y, Sun H, et al. A ship rotation detection model in remote sensing images based on feature fusion pyramid network and deep reinforcement learning. *Remote Sensing* 2018;10(12):1922.
88. Gao L, He Y, Sun X, et al. Incorporating negative sample training for ship detection based on deep learning. *Sensors* 2019;19(3):684.
89. Yan Y, Tan Z, Su N. A data augmentation strategy based on simulated samples for ship detection in RGB remote sensing images. *ISPRS International Journal of Geo-Information* 2019;8(6):276.
90. Wang M, Chen J-Y, Wang G, et al. High resolution remote sensing image ship target detection technology based on deep learning. *Optoelectronics Letters* 2019;15(5):391–5.
91. You Y, Cao J, Zhang Y, et al. Nearshore ship detection on high-resolution remote sensing image via scene-mask R-CNN. *IEEE Access* 2019;7:128431–44.
92. Nie X, Duan M, Ding H, et al. Attention mask R-CNN for ship detection and segmentation from remote sensing images. *IEEE Access* 2020;8:9325–34.
93. Chen Y, Li Y, Wang J, et al. Remote sensing image ship detection under complex sea conditions based on deep semantic segmentation. *Remote Sensing* 2020;12(4):625.
94. Guo H, Yang X, Wang N, et al. A rotational libra R-CNN method for ship detection. *IEEE Transactions on Geoscience and Remote Sensing* 2020;58(8):1–10.
95. Liu L, Bai Y, Li Y. Locality-aware rotated ship detection in high-resolution remote sensing imagery based on multi-scale convolutional network [Internet] [updated 2020 Jul 24; cited 2020 Jul 30] Available from: <<https://arxiv.org/abs/2007.12326>> .
96. Li M, Guo W, Zhang Z, et al. Rotated region based fully convolutional network for ship detection. *IGARSS 2018 - 2018 IEEE international geoscience and remote sensing symposium*; 2018 Jul 22-27; Valencia, Spain. Piscataway: IEEE Press; 2018.
97. Feng Y, Diao W, Sun X, et al. Towards automated ship detection and category recognition from high-resolution aerial images. *Remote Sensing* 2019;11:1901.
98. Simonyan K, Zisserman A. Very deep convolutional networks for large-scale image recognition [Internet] [updated 2014 Sep 4; cited 2020 Jul 30] Available from: <<https://arxiv.org/abs/1409.1556>> .
99. Nie G, Zhang P, Niu X, et al. Ship detection using transfer learned single shot multi box detector. *ITM Web Conference*, 2017, 01006.
100. Zhang Z, Guo W, Zhu S, et al. Toward arbitrary-oriented ship detection with rotated region proposal and discrimination networks. *IEEE Geoscience and Remote Sensing Letters* 2018;15(11):1745–9.
101. Ma X, Li W, Shi Z. Attention-based convolutional networks for ship detection in high-resolution remote sensing images. In: Lai JH, editor. *Pattern Recognition and Computer Vision. PRCV 2018: Pattern Recognition and Computer Vision*; 2018 Nov 23-26; Guangzhou, China. Cham: Springer International Publishing; 2018.
102. Wu Y, Ma W, Gong M, et al. A coarse-to-fine network for ship detection in optical remote sensing images. *Remote Sensing* 2020;12(2):246.
103. Tian T, Pan Z, Tan X, et al. Arbitrary-oriented inshore ship detection based on multi-scale feature fusion and contextual pooling on rotation region proposals. *Remote Sensing* 2020;12(2):339.
104. Tan X, Tian T, Li H. Inshore ship detection based on improved faster R-CNN. *Proceedings of SPIE 11429, MIPPR 2019: Automatic target recognition and navigation, eleventh international symposium on multispectral image processing and pattern recognition*; Wuhan, China. Bellingham: SPIE; 2020.
105. Li L, Zhou Z, Wang B, et al. A novel CNN-based method for accurate ship detection in HR optical remote sensing images via rotated bounding box [Internet]. [updated 2020 Apr 24; cited 2020 Jul 30]. Available from: <<https://arxiv.org/abs/2004.07124>> .
106. Lin T, Dollár P, Girshick R, et al. Feature pyramid networks for object detection. *2017 IEEE conference on Computer Vision and Pattern Recognition (CVPR)*; 2017 Jul 21-26; Honolulu, USA. IEEE Press: Piscataway; 2017.
107. Nie M, Zhang J, Zhang X. Ship segmentation and orientation estimation using keypoints detection and voting mechanism in remote sensing images. In: Lu H, Tang H, Wang Z, editors. *Advances in Neural Network-ISSN 2019. ISSN 2019: Advances in neural networks-ISSN 2019*; 2019 Jul 10-12; Moscow, Russia. Cham: Springer International Publishing; 2019.
108. Yao Y, Jiang Z, Zhang H, et al. Ship detection in optical remote sensing images based on deep convolutional neural networks. *Journal of Applied Remote Sensing* 2017;11(4) 042611.
109. Zhang S, Wu R, Xu K, et al. R-CNN-based ship detection from high resolution remote sensing imagery. *Remote Sensing* 2019;11(6):631.
110. He K, Gkioxari G, Dollár P, et al. Mask R-CNN. *2017 IEEE International Conference on Computer Vision (ICCV)*; 2017 Oct 22-29; Venice, Italy. Piscataway: IEEE Press; 2017.



111. Zhang Z, Li H, Zhang G, et al. CCNet: a high-speed cascaded convolutional neural network for ship detection with multispectral images. *Journal of Infrared and Millimeter Waves* 2019;**38**(3):290–5.
112. Girshick R. Fast R-CNN. *2015 IEEE International Conference on Computer Vision (ICCV); 2015 Dec 7-13; Santiago, Chile*. Piscataway: IEEE Press; 2015.
113. Wu F, Zhou Z, Wang B, et al. Inshore ship detection based on convolutional neural network in optical satellite images. *IEEE Journal of Selected Topics in Applied Earth Observations and Remote Sensing* 2018;**11**(11):4005–15.
114. Liu Z, Hu J, Weng L, et al. Rotated region based CNN for ship detection. *2017 IEEE International Conference on Image Processing (ICIP); 2017 Sep 17-20; Beijing, China*. Piscataway: IEEE Press; 2017.
115. Liu W, Ma L, Chen H. Arbitrary-oriented ship detection framework in optical remote-sensing images. *IEEE Geoscience and Remote Sensing Letters* 2018;**15**(6):937–41.
116. Zhang Y, Sheng W, Jiang J, et al. Priority branches for ship detection in optical remote sensing images. *Remote Sensing* 2020;**12**(7):1196.
117. Liu Z, Liu Y, Weng L, et al. A high resolution optical satellite image dataset for ship recognition and some new baselines. *6th international conference on pattern recognition applications and methods; 2017 Feb 24-26; Porto, Portugal*. SciTePress; 2017.
118. Chen K, Wu M, Liu J, et al. FGSD: A dataset for fine-grained ship detection in high resolution satellite images [Internet] [updated 2020 Mar 15; cited 2020 Jul 30] Available from: <<https://arxiv.org/abs/2003.06832>>.
119. Li Q, Mou L, Liu Q, et al. HSF-Net: Multiscale deep feature embedding for ship detection in optical remote sensing imagery. *IEEE Transactions on Geoscience and Remote Sensing* 2018;**56**(12):1–15.
120. Joseph S, Sasikala J, Juliet D. A novel vessel detection and classification algorithm using a deep learning neural network model with morphological processing (M-DLNN). *Soft Computing* 2019;**23**(8):2693–700.
121. Gallego A, Pertusa A, Gil P. Automatic ship classification from optical aerial images with convolutional neural networks. *Remote Sensing* 2018;**10**(4):511.
122. Rainey K, Stastny J. Object recognition in ocean imagery using feature selection and compressive sensing. *2011 IEEE Applied Imagery Pattern Recognition Workshop (AIPR); 2011 Oct 11-13; Washington, USA*. Piscataway: IEEE Press; 2011.
123. Rainey K, Parameswaran S, Harguess J, et al. Vessel classification in overhead satellite imagery using learned dictionaries. *Proceedings of SPIE 8499, applications of digital image processing XXXV, SPIE optical engineering + applications; 2012 Oct 15; San Diego, USA*. Bellingham: SPIE; 2012.
124. Huang L, Li W, Chen C, et al. Multiple features learning for ship classification in optical imagery. *Multimedia Tools and Applications* 2018;**77**(11):13363–89.
125. Shi Q, Li W, Tao R. 2D-DFrFT based deep network for ship classification in remote sensing imagery. *2018 10th IAPR workshop on Pattern Recognition in Remote Sensing (PRRS); 2018 Aug 19-20; Beijing, China*. Piscataway: IEEE Press; 2018.
126. Parameswaran S, Rainey K. Vessel classification in overhead satellite imagery using weighted “bag of visual words”. *Proceedings of SPIE 9476, automatic target recognition XXV, SPIE defense + security; 2015 May 22; Baltimore, USA*. Bellingham: SPIE; 2015.
127. Shi Q, Li W, Zhang F, et al. Deep CNN with multi-scale rotation invariance features for ship classification. *IEEE Access* 2018;**6**:38656–68.
128. Izmailov R, Bassu D, McIntosh A, et al. Application of multi-scale singular vector decomposition to vessel classification in overhead satellite imagery. *Proceedings of SPIE 9631, Seventh International Conference on Digital Image Processing (ICDIP 2015); Los Angeles, USA*. Bellingham: SPIE; 2015.
129. Grasso R. Ship classification from multi-spectral satellite imaging by convolutional neural networks. *2019 27th European Signal Processing Conference (EUSIPCO); 2019 Sep 2-6; A Coruna, Spain*. Piscataway: IEEE Press; 2019.
130. Liu Y, Cui H, Li G. A novel method for ship detection and classification on remote sensing images. In: Lintas A, Rovetta S, Verschure P, editors. *Artificial neural networks and machine learning-ICANN 2017. ICANN 2017: Artificial Neural Networks and Machine Learning-ICANN 2017; 2017 Sep 11-14; Alghero, Italy*. Cham: Springer International Publishing; 2017.
131. Li W, Fu K, Sun H, et al. Integrated localization and recognition for inshore ships in large scene remote sensing images. *IEEE Geoscience and Remote Sensing Letters* 2017;**14**(6):936–40.
132. Luu V, Dinh V, Luong N, et al. Improving the bag-of-words model with Spatial Pyramid matching using data augmentation for fine-grained arbitrary-oriented ship classification. *Remote Sensing Letters* 2019;**10**:826–34.
133. Guo Z, Zhang L, Zhang D. A completed modeling of local binary pattern operator for texture classification. *IEEE Transactions on Image Processing* 2010;**19**(6):1657–63.
134. Clausi D, Jernigan M. Designing Gabor filters for optimal texture separability. *Pattern Recognition* 2000;**33**:1835–49.
135. Cheng G, Han J, Zhou P, et al. Multi-class geospatial object detection and geographic image classification based on collection of part detectors. *ISPRS Journal of Photogrammetry and Remote Sensing* 2014;**98**:119–32.
136. Cheng G, Han J, Lu X. Remote sensing image scene classification: Benchmark and state of the art. *Proceedings of the IEEE* 2017;**105**(10):1865–83.
137. Kaggle. Airbus ship detection challenge [Internet] Available from: <<https://www.kaggle.com/c/airbus-ship-detection/data>>.
138. Lam D, Kuzma R, McGee K, et al. xView: Objects in context in overhead imagery [Internet] [updated 2018 Feb 22; cited 2020 Jul 30] Available from: <<https://arxiv.org/abs/1802.07856>>.
139. Xia G, Bai X, Ding J, et al. DOTA: A large-scale dataset for object detection in aerial images. *2018 IEEE/CVF conference on computer vision and pattern recognition; 2018 Jun 18-23; Salt Lake City, USA*. Piscataway: IEEE Press; 2018.
140. Zhang Y, Yuan Y, Feng Y, et al. Hierarchical and robust convolutional neural network for very high-resolution remote sensing object detection. *IEEE Transactions on Geoscience and Remote Sensing* 2019;**57**(8):5535–48.
141. Li K, Wan G, Cheng G, et al. Object detection in optical remote sensing images: a survey and a new benchmark. *ISPRS Journal of Photogrammetry and Remote Sensing* 2020;**159**:296–307.
142. Chen Y, Zheng J, Zhou Z. Airbus ship detection-traditional vs convolutional neural network approach. Available from: <<http://cs229.stanford.edu/proj2018/report/58.pdf>>.
143. Ding J, Xue N, Long Y, et al. Learning RoI transformer for oriented object detection in aerial images. *2019 IEEE/CVF Conference on Computer Vision and Pattern Recognition (CVPR); 2019 Jun 15-20; Long Beach, USA*. Piscataway: IEEE Press; 2019.
144. Girshick R, Donahue J, Darrell T, et al. Rich feature hierarchies for accurate object detection and semantic segmentation. *2014 IEEE conference on computer vision and pattern recognition; 2014 Jun 3-28; Columbus, USA*. Piscataway: IEEE Press; 2014.
145. Liao M, Zhu Z, Shi B, et al. Rotation-sensitive regression for oriented scene text detection. *2018 IEEE/CVF conference on computer vision and pattern recognition; 2018 Jun 18-23; Salt Lake City, USA*. Piscataway: IEEE Press; 2018.
146. Park K, Park J, Jang J, et al. Multi-spectral ship detection using optical, hyperspectral, and microwave SAR remote sensing for sustainability of the coastal region. *Sustainability* 2018;**10**:4064.

147. Kanjir U, Greidanus H, Oştir K. Vessel detection and classification from spaceborne optical images: a literature survey. *Remote Sensing of Environment* 2018;**207**:1–26.
148. Willhauck G, Caliz J, Hoffmann C, et al. Object oriented ship detection from VHR satellite images. *Processing 6th geomatic week conference; Barcelona, Spain*, 2005.
149. Hong Z, Jiang Q, Guan H, et al. Measuring overlap-rate in hierarchical cluster merging for image segmentation and ship detection. *Fourth international conference on Fuzzy Systems and Knowledge Discovery (FSKD 2007); 2007 Aug 24-27; Haikou, China*. Piscataway: IEEE Press; 2007.
150. Pegler K, Coleman D, Pelot R, et al. An enhanced spatio-spectral template for automatic small recreational vessel detection. *Photogrammetric Engineering and Remote Sensing* 2007;**73** (1):79–87.
151. Antelo J, Ambrosio G, Gonzalez J, et al. Ship detection and recognition in high-resolution satellite images. *2009 IEEE international geoscience and remote sensing symposium; 2009 Jul 12-17; Cape Town, South Africa*. Piscataway: IEEE Press; 2009.
152. Peng C, Huang W, Shi A, et al. Automatic ship detection in HJ-1A satellite data. *Proceedings of SPIE 7495, MIPPR 2009: Automatic target recognition and image analysis, sixth international symposium on multispectral image processing and pattern recognition; 2009 Oct 30; Yichang, China*. Bellingham: SPIE; 2009.
153. Yang G, Lu Q, Gao F. A novel ship detection method based on sea state analysis from optical imagery.. *2011 Sixth international conference on image and graphics; 2011 Aug 12-15; Hefei, China*. Piscataway: IEEE Press; 2011.
154. Johansson P. Small vessel detection in high quality optical satellite imagery. Sweden: Chalmers University of Technology; 2011.
155. Saur G, Estable S, Zielinski K, et al. Detection and classification of man-made offshore objects in TerraSAR-X and RapidEye imagery: selected results of the DeMarine-DEKO project. *OCEANS 2011 IEEE - Spain; 2011 Jun 6-9; Santander, Spain*. Piscataway: IEEE Press; 2011.
156. Xu J, Fu K, Sun X. An invariant generalized hough transform based method of inshore ships detection. *2011 international symposium on image and data fusion; 2011 Aug 9-11; Tengchong, China*. Piscataway: IEEE Press; 2011.
157. Xu J, Sun X, Zhang D, et al. Automatic detection of inshore ships in high-resolution remote sensing images using robust invariant generalized hough transform. *IEEE Geoscience and Remote Sensing Letters* 2014;**11**(12):2070–4.
158. Guo W, Xia X, Wang X. Variational approximate inferential probability generative model for ship recognition using remote sensing data. *Optik* 2015;**126**(23):4004–13.
159. Pan B, Jiang Z, Wu J, et al. Ship recognition based on active learning and composite kernel SVM. In: Tan T, Ruan Q, Wang S, editors. *IGTA 2015: Advances in Image and Graphics Technologies; 2015 Jun 19–20; Beijing, China*. Berlin: Springer; 2015.
160. Xing Q, Meng R, Lou M, et al. Remote sensing of ships and offshore oil platforms and mapping the marine oil spill risk source in the bohai sea. *Aquatic Procedia* 2015;**3**:127–32.
161. Yokoya N, Iwasaki A. Object detection based on sparse representation and Hough voting for optical remote sensing imagery. *IEEE Journal of Selected Topics in Applied Earth Observations and Remote Sensing* 2015;**8**(5):2053–62.
162. Negula I, Poenaru V, Olteanu V, et al. SENTINEL-1/2 data for ship traffic monitoring on the danube river *ISPRS - International Archives of the Photogrammetry, Remote Sensing and Spatial Information Sciences*. p. 37–41.
163. Zhang R, Yao J, Zhang K, et al. S-CNN-based ship detection from high-resolution remote sensing images *ISPRS - International Archives of the Photogrammetry, Remote Sensing and Spatial Information Sciences*. p. 423–30.
164. Rainey K, Reeder J, Corelli A. Convolution neural networks for ship type recognition. *Proceedings of SPIE 9844, Automatic target recognition XXVI, SPIE defense + security; 2016 May 12; Baltimore, USA*. Bellingham: SPIE; 2016.
165. Liu Z, Wang H, Weng L, et al. Ship rotated bounding box space for ship extraction from high-resolution optical satellite images with complex backgrounds. *IEEE Geoscience and Remote Sensing Letters* 2016;**13**(8):1074–8.
166. Gianinetto M, Aiello M, Marchesi A, et al. OBIA ship detection with multispectral and SAR images: A simulation for Copernicus security applications. *2016 IEEE International Geoscience and Remote Sensing Symposium (IGARSS); 2016 Jul 10-15; Beijing, China*. Piscataway: IEEE Press; 2016.
167. Huang S, Xu H, Xia X. Active deep belief networks for ship recognition based on BvSB. *Optik* 2016;**127**(24):11688–97.
168. Li N, Zhang Q, Zhao H, et al. Ship detection in high spatial resolution remote sensing image based on improved sea-land segmentation. *Proceedings of SPIE 10156, hyperspectral remote sensing applications and environmental monitoring and safety testing technology; 2016 Oct 25; Beijing, China*. Bellingham: SPIE; 2016.
169. Li X, Xie W, Wang L, et al. Ship detection based on surface fitting modeling for large range background of ocean images. *2016 IEEE 13th International Conference on Signal Processing (ICSP); 2016 Nov 6-10; Chengdu, China*. Piscataway: IEEE Press; 2016.
170. Liu Y, Yao L, Xiong W, et al. Fusion detection of ship targets in low resolution multi-spectral images. *2016 IEEE International Geoscience and Remote Sensing Symposium (IGARSS); 2016 Jul 10-15; Beijing, China*. Piscataway: IEEE Press; 2016.
171. Toppito F, Massari M, Lombardi R, et al. Space shepherd-using space systems to save human lives. Available from: <[https://re.public.polimi.it/retrieve/handle/11311/980310/116214/report\\_16-01.pdf](https://re.public.polimi.it/retrieve/handle/11311/980310/116214/report_16-01.pdf)> .
172. Wang H, Zhu M, Lin C, et al. Ship detection in optical remote sensing image based on visual saliency and AdaBoost classifier. *Optoelectronics Letters* 2017;**13**(2):151–5.
173. He H, Lin Y, Chen F, et al. Inshore ship detection in remote sensing images via weighted pose voting. *IEEE Transactions on Geoscience and Remote Sensing* 2017;**55**(6):3091–107.
174. Zhang Z, Shao Y, Tian W, et al. Application potential of GF-4 images for dynamic ship monitoring. *IEEE Geoscience and Remote Sensing Letters* 2017;**14**(6):911–5.
175. Nie T, He B, Bi G, et al. A method of ship detection under complex background. *ISPRS International Journal of Geo-Information* 2017;**6**(6):159.
176. Bi F, Chen J, Zhuang Y, et al. A decision mixture model-based method for inshore ship detection using high-resolution remote sensing images. *Sensors* 2017;**17**(7):1470.
177. Yamamoto T, Kazama Y. Ship detection leveraging deep neural networks in WorldView-2 images. *Proceedings of SPIE 10427, image and signal processing for remote sensing XXIII, SPIE remote sensing; 2017 Oct 4; Warsaw, Poland*. Bellingham: SPIE; 2017.
178. Xu F, Liu J, Dong C, et al. Ship detection in optical remote sensing images based on wavelet transform and multi-level false alarm identification. *Remote Sensing* 2017;**9**(10):985.
179. Lin H, Shi Z, Zou Z. Maritime semantic labeling of optical remote sensing images with multi-scale fully convolutional network. *Remote Sensing* 2017;**9**:480.
180. Willburger K, Schwenk K. Using the time shift in single pushbroom datatakes to detect ships and their heading. *Proceedings of SPIE 10427, image and signal processing for remote sensing XXIII, SPIE remote sensing; 2017 Oct 4; Warsaw, Poland*. Bellingham: SPIE; 2017.
181. Dong C, Liu J, Xu F. Ship detection in optical remote sensing images based on saliency and a rotation-invariant descriptor. *Remote Sensing* 2018;**10**(3):400.

182. Song M, Qu H, Zhang G, et al. Detection of small ship targets from an optical remote sensing image. *Frontiers of Optoelectronics* 2018;**11**(3):275–84.
183. Wang L, Pei J, Xie W, et al. Ship detection using STFT sea background statistical modeling for large-scale oceansat remote sensing image. *Proceedings of SPIE 10611, MIPPR 2017: Remote sensing image processing, geographics information systems, and other applications, tenth international symposium on multispectral image processing and pattern recognition; 2018 Mar 8; Xiangyang, China*. Bellingham: SPIE; 2018.
184. Luu V, Luong N, Bui Q, et al. Robust anomaly-based ship proposals detection from pan-sharpened high-resolution satellite image [Internet] [updated 2018 Apr 25; cited 2020 Jul 30] Available from: <<https://arxiv.org/abs/1804.09322>>.
185. Liu Y, Yao L, Xiong W, et al. GF-4 satellite and automatic identification system data fusion for ship tracking. *IEEE Geoscience and Remote Sensing Letters* 2018;**16**(2):281–5.
186. Yu Y, Ai H, He X, et al. Ship detection in optical satellite images using haar-like features and periphery-cropped neural networks. *IEEE Access* 2018;**6**:71122–31.
187. Kanjir U. Detecting migrant vessels in the Mediterranean Sea: using Sentinel-2 images to aid humanitarian actions. *Acta Astronautica* 2019;**155**:45–50.
188. Li H, Chen L, Li F, et al. Ship detection and tracking method for satellite video based on multiscale saliency and surrounding contrast analysis. *Journal of Applied Remote Sensing* 2019;**13**(2) 026511.
189. Chen H, Gao T, Chen W, et al. Contour refinement and EG-GHT-based inshore ship detection in optical remote Sensing Image. *IEEE Transactions on Geoscience and Remote Sensing* 2019;**57**(11):8458–78.
190. Chen J, Xie F, Lu Y, et al. Finding arbitrary-oriented ships from remote sensing images using corner detection. *IEEE Geoscience and Remote Sensing Letters* 2019;1–5.
191. Nina W, Condori W, Machaca V, et al. Small ship detection on optical satellite imagery with YOLO and YOLT2020. In: Arai K, Kapoor S, Bhatia R, editors. *FICC 2020: Advances in information and communication; 2020 Mar 5; San Francisco, USA*. Cham: Springer International Publishing; 2020.
192. Wang B, Huang C, Tao J, et al. Interpreting deep convolutional neural network classification results indirectly through the preprocessing feature fusion method in ship image classification. *Journal of Applied Remote Sensing* 2020;**14**(1) 016510.
193. Uçar F, Korkmaz D. A ship detector design based on deep convolutional neural networks for satellite images. *Sakarya University Journal of Science* 2020;**24**:197–204.
194. Ji K, Chen Z, Jiang Z, et al. Accurate bounding box for ship detection on remote sensing images with complex background. *Proceedings of SPIE 11432, MIPPR 2019: Remote sensing image processing, geographic information systems, and other applications, eleventh international symposium on multispectral image processing and pattern recognition; 2020 Feb 14; Wuhan, China*. Bellingham: SPIE; 2020.
195. Cramer M. The DGPF-test on digital airborne camera evaluation – overview and test design. *Photogrammetrie - Fernerkundung - Geoinformation* 2010;**2010**(2):73–82.